Heliyon 9 (2023) e15721

Contents lists available at ScienceDirect

Heliyon

journal homepage: www.cell.com/heliyon

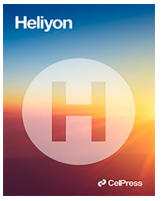

Research article

Production, optimization, and characterization of Ethiopian variant Prosopis juliflora based biodiesel

Hailu Abebe Debella [a,*], Venkata Ramayya Ancha [b], Samson Mekbib Atnaw [a]

[a] Addis Ababa Science and Technology University, College of Mechanical and Electrical Engineering, Addis Ababa, P. B. No. 16417, Ethiopia
[b] Faculty of Mechanical Engineering, Institute of Technology, Jimma University, P.O. Box: 378, Jimma, Ethiopia

ARTICLE INFO

Keywords:
Prosopis juliflora
Rheology
Biodiesel
Characterization
Optimization

ABSTRACT

Considering the need for biodiesel production from non-edible oil sources and taking into account the fact that Prosopis Juliflora (JF) is identified as a highly invasive species in Ethiopia, this research focuses on biodiesel production from a possible and promising alternative feedstock. The objective of this study is to analyze Ethiopian variant Juliflora based biodiesel (JFB) production through transesterification, carry out optimization by exploring the effects of various process parameters and characterization of functional groups (with GC-MS,FT-IR and NMR) including rheological behavior, not yet been reported earlier. As per ASTM protocol testing, the methyl ester of Juliflora has been found to have the following main fuel properties: kinematic viscosity (mm^2/s) 3.395, cetane number 52.9, acid number (mgkoh/g) 0.28, density (gm/ml) 0.880, calorific value (MJ/kg) 44.4, methyl ester content (%) 99.8, and flashpoint (°C) 128, copper strip corrosion value 1a,%FFA (free fatty acid) 0.14. When compared with those of diesel, the viscosity, density, and flash point of JFB are seen to be higher than those of diesel, although it has a similar calorific value but more importantly higher than most of the other biodiesels. Based on an assessment using response surface methodology, methanol concentration together with catalyst loading, temperature, and reaction time are determined to be the most important influencing process parameters. The best molar ratio for methanolysis was observed to be 6:1 with a catalyst concentration of 0.5 wt% at 55 °C for 60 min for biodiesel yield at 65%. The JFB maximum yield of 130 ml at 70 min and the minimum yield of 40 ml at 10 min demonstrate that as mixing time increases, JFB yield tend to increase up to a certain time limit. The maximum raw oil yield rom crushed seed with hexane solvent was observed to be 480 ml within 3 days from 2.5 kg of crushed seed. The Fourier transform infrared analysis (FT-IR) revealed the presence of all desired functional groups necessary for biodiesel on OH radicals at wave numbers of 3314.40 cm^{-1}, Aliphatic methyl C–H at 2942.48 cm^{-1} with a functional group (CH-3-,-CH2-), and methylene C–H at 2832.59 cm^{-1}. The gas chromatography-mass spectrometer (GC–MS) study confirmed the higher ester content present in the JFB with a higher unsaturation level of 68.81%. The fatty acid, oleic acid has a lower saturation level of 4.5%, while palmitic acid has a lower threshold level of 2.08%. The Rheometer test showed that shear stress and viscosity reduced with increasing temperature within the range of biodiesel requirements, and the Newtonian behavior was confirmed. The JFB has a fairly high viscosity and shear rate at low temperatures. The ^1H NMR (nuclear magnetic resonance) study established that JFB has a necessary ingredient; and aliphatic resonances occur in the chemical shift region of 1.5–3.0 ppm. Significant regions indicate protons bound to heteroaromatics, aldehydes, as shown by ^{13}C NMR spectrum. The findings from the FT-

* Corresponding author.
E-mail address: hailu.abebe@aastu.edu.et (H.A. Debella).

https://doi.org/10.1016/j.heliyon.2023.e15721
Received 19 July 2022; Received in revised form 11 April 2023; Accepted 19 April 2023
Available online 23 April 2023

IR, GC-MS, ^{1}H NMR, and ^{13}C NMR are in agreement thus validating the presence of numerous functional groups in JFB as such. Since JFB possesses the requisite biodiesel fuel attributes, Prosopis Juliflora need to be pursued as a promising biodiesel feedstock in Ethiopia for alleviating the burden of imported fuels while also addressing difficulties with emissions released by the combustion of fossil fuels.

1. Introduction

Long-term development requires an energy supply derived from renewable biofuels. Biodiesel, biomass, biogas, and synthetic fuels are examples of alternative fuel sources being explored across the world. Biodiesel is one of them that can be utilized straight away, while others require some tweaking before they can be used in place of traditional fuels [1]. It may be made in a variety of ways, including thermal and chemical methods. Transesterification, heat cracking, and micro emulsion have all been mentioned as popular biodiesel manufacturing processes. Transesterification and thermal cracking are two of the most popular methods for producing biodiesel. However, the transesterification-based biodiesel synthesis is more attractive, whereby vegetable oil or fat combines with alcohol to create alkyl-esters utilizing a catalyst [2]. The process of transesterification using methanol, ethanol, propanol, and butanol is the most appropriate. The yield is determined by the amount of fatty acid available, water, temperature, catalyst, and time during the esterification process. The output of biodiesel might vary by up to 96% depending on the aforementioned parameter [3]. Transesterification of ethanol or methanol using sodium hydroxide (NaOH) or potassium hydroxide (KOH) as a catalyst has been utilized by the majority of researchers to produce biodiesel Because of its better characteristics and lower cost, methanol is the most often utilized alcohol in the esterification process. Because of its high conversion rate, a homogeneous basic catalyst is utilized in traditional biodiesel manufacturing. NaOH is chosen among these catalysts because of its efficiency and low cost in this process. The amount of catalyst required is determined by the acid number of the oil. Lower viscosity, greater calorific value, and enhanced cetane number are some of the characteristics gained by biodiesel [4].

Ethiopia, a nation in the sub-Saharan region of Africa with a topography of 1.1 million km^2, has the second-highest demographic in the continent after Nigeria, with over 46 million people living without electricity in the country's rural areas [5]. The complete reliance on traditional biomass including firewood, crop waste, animal dung, and charcoal further highlights the energy poverty of the nation. More than 95% of the country's energy demand is met by energy produced from indigenous bioenergy, which is also used by well over 86.42% of rural families [6]. Regrettably, producing energy from traditional bio resources is neither environmentally friendly nor sustainable. Significant deforestation, desertification, and emissions of greenhouse gases have been brought on by a heavy reliance on indigenous biomass [7]. Conversely, oil imports are the only source of fuel for the Ethiopian transportation sector, with an estimated annual cost of almost US$ 3 billion [8]. The increased demand for foreign currency along with the rise and fluctuation in the price of petroleum has harmed the national economy. Additionally, it has been determined that using and producing energy from traditional carbon-based fuels like coal, natural gas, and petroleum are the main contributors to emissions of greenhouse gases [9,10]. Therefore, many researchers were interested in investigating alternative energy sources for producing heat and electricity, such as wind and hydropower. Alternatively, a variety of biofuels might replace petroleum-based fuels like diesel and gasoline, which are mostly used in the transportation sector. Biodiesel has been recognized as a biofuel that can be used for a variety of diesel engine purposes [11]. To provide sufficient feedstock that does not conflict with the production of food and fodder, it is necessary to make the switch to these alternative energies.

Numerous varieties of non-food flora have just been identified in Ethiopia that can be used to make biodiesel. The most commonly recognized feedstocks include Jatropha curcas L (J. curcas), Castor bean, Pongamia, Candlenut, and Croton seeds [6]. Juliflora seed has not been used yet as a biodiesel source even though the country has large potential in this regard.

To maximize the management of the oil yield Since the conventional method of oil extraction and optimization technique time appears to be laborious, ineffective, and resource intensive in terms of time and resources, scientific optimization technique is preferred for the extraction process by using a suitable solvent and catalyst as well as an exact reaction time in order to reduce unnecessary cost, resource, and time wastage [12]. According to the conventional method, one variable will be optimized while the other variables are kept constant, and a significant number of experimental runs are required to assess the impact of a single element [12]. Also, it doesn't guarantee the best level of each individual variable and the interaction between them [4]. Over the years, the use of response surface methodology has been one strategy used to overcome these issues (RSM). RSM has been used successfully in a number of research, including the extraction of seed oils from Algae mamelos [12], Argemone Mexicana [13], Litopenaeus vannamei waste [14], Carcia papaya [15], Micro algal [16], Australian native stone fruit [17] and waste frying [18].

In view of the gap identified above, the goal of this study is to look into the production and optimization of biodiesel generated from JFB using single-step transesterification, which will be followed by a study of the fuel's characteristics. Transesterification of Juliflora seed oil with methanol as a solvent and NaOH as a catalyst produces Juliflora methyl ester. To understand the thermal behavior and evaluate the chemical composition, the biodiesel's many physical and chemical characteristics were assessed. Gas chromatography-mass spectrometry (GC-MS) was used to determine the chemical components of Juliflora oil methyl ester (JFOME). Fourier transform infrared (FT-IR) was used to study the hydrocarbon functional groups present on JFB (B100). The constituent compounds of JFB were analyzed ^{H}1NMR and ^{13}CNMR, The rheometer technique was also employed to assess the influence of temperature on B100 viscosity and shear stress. JFB's pH value with additives was determined. To maximize oil extraction from Prosopis juliflora seeds using RSM to produce biodiesel was used to assess the influence of solvent concentration, catalyst concentration, and temperature on

biodiesel optimum yield. The effect of agitation time on the maceration of hexane on crude oil yield was studied during crude oil extraction from JF-seed, and the effect of reaction time on biodiesel yield was investigated. The variables under investigation were temperature, time, solvent concentration, and catalyst concentration. Also, RSM's performance assessment for oil extraction was contrasted. The relative significance of the process parameters was also established.

1.1. The novelty of the work

Juliflora based biodiesel was previously produced, with various solvent concentrations of methanol, NaOH catalyst with various reaction times and temperature variations, even though no study has been conducted on Ethiopian variant A few of the works in literature addressed some of the key properties for using JFB as a biodiesel in diesel engine applications. Among all, most of the studies focused on properties like Cetane number, calorific value, density, viscosity, fire point, and flash point as shown in Refs. [19–25] As a result, the current study focuses on new properties in addition to those mentioned in the literature, such as cloud point, pour point, density (at two temperatures), specific gravity, saponification value, iodine number, copper strip corrosion test, acid number, free fatty acid (FFA), total glycerin, pH value, methyl ester content, fuel composition and characterization for functional groups present, water, and sediment content. The rheological analysis on JFB to reveal the impacts of temperature and shear rate on dynamic viscosity and shear stress fluctuations, not yet reported, has been carried out as another key and major part in this work. Previous studies characterized the fatty acid compositions for JFB as shown in Ref. [24], but some differences in feedstock variants for the JFB seed, the soil effect etc. might reveal deviations related to the types of unsaturated and saturated fatty acid compositions and need to be characterized before usage in the engine. This study has been carried out to address the lacunae highlighted earlier involving JFB production, optimization and characterization involving GC-MS, FT-IR, NMR and rheological testing.

2. Materials and methods

2.1. Materials

The materials and chemicals were chosen based on their ease of procurement and appropriateness. JF oil was chosen as a feedstock for biodiesel production in this study, and it was gathered in Ethiopia's Afar region Metahara and Awash woreda, which has a scorching environment. The commercially available petroleum-based diesel fuel was obtained from a local petroleum supply oil company in Addis Ababa, Ethiopia. The fuel properties of diesel fuel comply with EN 590, as confirmed by Ethiopia's national petroleum ministry. Methanol (99.9% purity) as short-chain alcohol, NaOH pellets (99% purity) as an alkali catalyst, and hexane (99.5% purity) for JF oil extraction. The reference standards for fatty acid methyl esters were obtained by examination of the JFB oil using a thermos-scientific instrument produced in the United States.

2.2. Feedstock for seed extraction

Prosopis juliflora is a South American, Central American, and Caribbean evergreen tree. It's known as mesquite in the United States. It grows quickly, fixes nitrogen, and can withstand dry conditions and salty soils. Prosopis juliflora may provide a range of useful commodities and services, including construction materials, charcoal, soil conservation, and the regeneration of damaged and salty soils, under the appropriate conditions. P. juliflora is a thorny plant that may be found in the hot climate regions of Ethiopia. It produces 2.5 tons of wood per hectare per year and includes over 70% hemicellulose fraction [26,27], which is known to improve the quality of bio-oils from biomass. P. juliflora has by now invaded approximately 1.7 million hectares of land at different cover levels (12,3% of the surface) and is expanding at a rate of 3.11×10^4 ha yr^{-1} [28, 29]. On average, it produces 5000 l/ha oil as indicated in Ref. [24]. In addition as [30] investigated fruit of the Prosopis juliflora looks nearly flat. About 1 foot long, 5–15 mm wide, and 3–9 mm thick, the pods have these dimensions. As they mature, the mature pods turn from green to mushy and yellowish-brown in color. There

Fig. 1. Prosopis juliflora plant (1. Prosopis, Juliflora tree, 2. Prosopis Juliflora pods, 3. Prosopis Juliflora seed).

are one to sixteen (pod) fruits in each inflorescence. 6.5 mm wide and weighing between 0.20 and 0.32 g (20,000–32000 seeds/kilogram), Seeds are small round objects. Based on the climatic conditions and ecology, kernels weighing 5 kg–10 kg per tree can be produced. At a density of around 20 kg/tree, Prosopis juliflora is predicted to produce 2230 kg/ha of pods. Because it is a non-food plant, it does not offer the same food security risks as other food crops (such as sugarcane, sorghum, and maize, which were previously utilized to produce bio-oils) [31]. Furthermore, P. juliflora is suspected of depleting ground aquifers in various regions of Ethiopia, to the point where the government of Ethiopia ordered the shrubs' entire abolition in the Afar and Oromia region in 2013 [28,29,32], As a result, we've chosen P. juliflora for this study because of its advantageous features for bio-oil production, as well as the fact that it may be used as an asset rather than a curse. Because the seeds are contained in indehiscent hard endocarp fruits, the Prosopis juliflora planting begins with the extraction of seeds from the pods. The seeds are readily extracted by cutting the pods lengthwise and crosswise between the seeds. Fig. 1 shows trees, pods, and seeds of Prosopis Juliflora.

2.3. Instrumentation

2.3.1. GC-MS

The JFB-oil sample was analyzed by GC-MS (Agilent 6890 N GC 5977MS) with electron ionization (EI) source, utilizing an inert column (NSP5 Inert 30 m × 0.25 mm x 0.25 μm), with a GC oven temperature program of 40–100 °C @2 °C/min, and 100–200°@20 °C/min. The EI MS parameters included a solvent delay of 2.10 min, a source temperature of 230 °C, and a scan range of 29–550 amu. GC He, purity 99.99%, is the carrier gas. Constant flow of 1 ml/min, inlet temperature of 250 °C, split ratio of 4:1, and injection volume of 1 μL.

2.3.2. FT-IR

For the FT-IR (Thermo fisher FTIR spectrometer-Nicolet iS50) analysis, at 4 cm^{-1} resolution with KBr as a background matrix in the range of 4000–400 cm^{-1}, were used to determine the various functional groups of JFB Identification were carried out using Spectrum iS50ABX spectrometer (Thermo-scientific, USA).

2.3.3. H^1-NMR and ^{13}CNMR

H^1-NMR and ^{13}C-NMR spectra of JFB-oil was recorded using a Bruker 400 MHz NMR Advance II with 5 mm PABBO probe. Deuterated methanol was used as the solvent in both ^{13}C-NMR and 1H-NMR. Sixteen and 16,385 scans were collected for H^1-NMR and ^{13}C-NMR, respectively.

2.3.4. pH 7110

pH value determination of JFB was carried out using pH7110 (inolab®, Germany) with pH accuracy (±0.005 + −0.01/0.1), with a measuring range mV (−1200.0 to + 1200/-2000 to+2000 mV).

2.3.5. Rheometer

The analysis of the effect of temperature and shear rate on viscosity and shear stresses of JFB was carried out using modular

Fig. 2. Preparation phases of juliflora seed (1. juliflora fruit, 2. juliflora seedpod, 3. Sun drying Process, 4. mechanical crushing, 5. fine crushing with electric grinder, 6. crushed seed powder collection).

compact Rheometer MCR102 SN82129736 (Anton Paar, Austria, Europe).

2.3.6. Software used

F095 Origin software version 9.8 was used to simplify the graphs used on the FT-IR and GC-MS instrument data to show the effect of temperature and shear rate on viscosity and the shear stress for JFB.

F095 Minitab statistical software version 20 was utilized for RSM (response surface methodology) for ANOVA (analysis of variance) analysis for the effect of temperature, catalyst, and solvent concentrations on JFB extraction were used.

2.4. Biodiesel production processes

2.4.1. Seed collection and preparation

2.4.1.1. Seed collection. Since all seedpods were utilized on a mechanical screw machine, seedpod collection and preparation are required a second time after mechanical extraction was not as successful. The seed was harvested and acquired once more from the hot temperature dry districts of Awash and Methahara in the Afar region, which is 227 km from Ethiopia's capital Addis Ababa. From 1 quintal by volume seedpod 60 kilos by weight-matured seedpods or (60%) were gathered from several seedpod trees.

2.4.1.2. Seed preparation. Fig. 2 from numbers 1 to 6. Depicts the collection, preparation, drying, and crushing of seedpods. The dried seedpod was first crushed by hand, as per the local and traditional method, to make it easier and simpler to ground using the electric machine grinder. After the seedpods were manually crushed and thoroughly prepared, they were ground again with a portable electric grinder. The powdered crushed Juliflora seedpod was now ready for maceration by the solvent. As a result, a finer, powder-like seedpod is created, suitable for simple reactivity and digestion by the solvent (Hexane).

2.5. Biodiesel extraction

2.5.1. Solvent oil existence checking sample extraction process

To enable mass manufacturing, two extraction steps were used for the oil. The first approach is sample-based extraction to check whether oil is there in the seedpod, while the second is batch extraction for mass production. The batch extraction technique generates more oil for a single batch procedure on a single container, whereas the sample-based extraction method is faster and saves time, but the oil output is low at a time. This can be used as a first step in determining whether a given sample seed contains oil or not before proceeding with the batch extraction procedure. As a result, each thimble contains 100 gm crushed powder and 150 ml hexane with 99.9% purity, as shown by experiments, [33]. As a result, the frequency of operation is too high to produce the required oil output. For example, only 25 ml of oil is created from a single operation or method, which is a little quantity when compared to batch extraction, but the test verifies that oil exists so that the next batch extraction process may be planned.

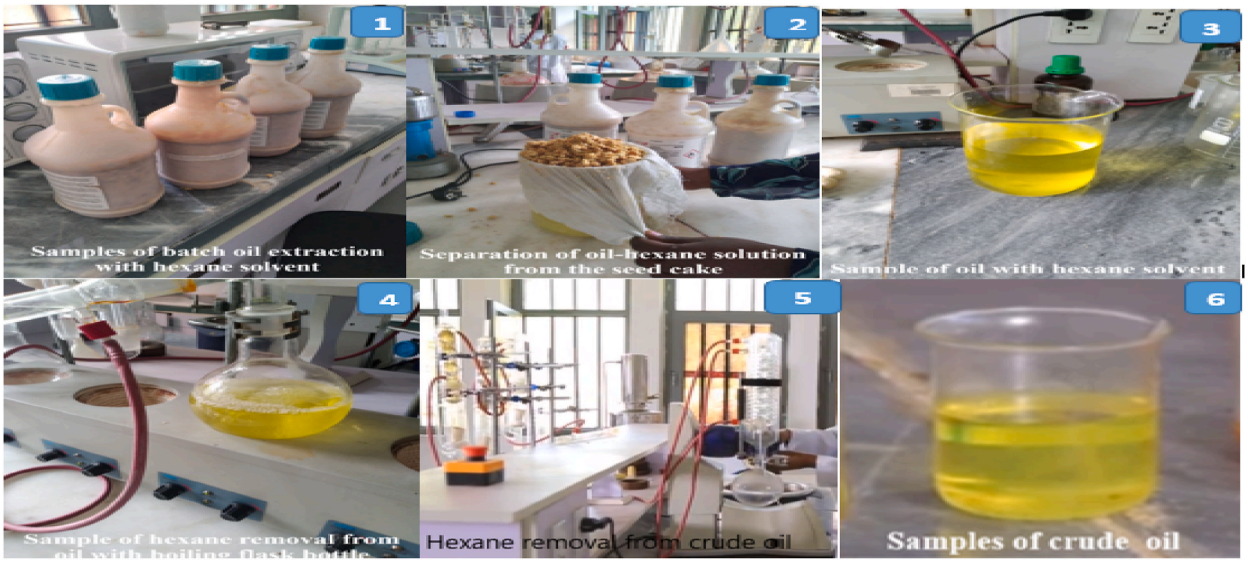

Fig. 3. Batch extraction (1. crushed seed with hexane, 2. crude oil and hexane separation from crushed seed, 3. oil sample with hexane, 4. process to remove hexane, 5. hexane collection, 6. pure crude oil sample).

2.5.2. Batch oil solvent extraction process

The batch Oil was extracted from Juliflora seedpods using *n*-hexane solvent in various bottles or batches. Each batch comprised 2 kilos of crushed powder seedpod and 2.5 litters of hexane, combined by a rotary mixer, and kept at room temperature for three days as the optimal period for improved digestion of the solution illustrated in Fig. 3, top. The seedpod powder is separated from the hexane solvent and crude oil in the second stage after it has been thoroughly combined and digested. By hand a thick cotton layer was used to separate the combined solution of hexane and crude oil from the hard seedpod cake (next), after which the crude oil with hexane falls and is ready to boil. Soxhlet device is used to separate pure crude oil from hexane solvent. There is no need to use a thimble with crushed seedpod samples; instead, combine the hexane and crude oil in a round bottom flask and heat at 50 °C until the hexane has evaporated completely, then condense in the Rota evaporator. Various studies have been conducted utilizing hexane as a solvent in a similar manner, such as [34–36].

Fig. 4 shows two circular bottom flasks on the bottom position of the rotary evaporator. Because they had distinct paths from the soxhlet chamber, the separate round bottom flask gathered both hexane solvent that was condensed on one side and crude oil on the other flask bottle. The golden-colored crude oil that has been separated from the hexane was then taken out or collected in a separate container. Finally, utilizing the Soxhlet oil extractor at Wondogenet Agriculture Research Center Laboratory, 6 L of crude oil (10%) could be recovered from 60 kg of PJF seedpods using solvent extraction method. The formula is shown in eq. (1)

The following formula was used to compute the crude oil yield:

$$\text{Yield } (\%) = \frac{\textbf{kilograms of crude oil}}{\textbf{kiligrams of seed}} \text{x}100 \tag{1}$$

2.6. Transesterification process for juliflora derived biodiesel

Trans-esterification, phase separation, washing, and drying, the most common steps in the biodiesel production process were performed and shown in Fig. 5. For the transesterification procedure, solvents and instruments such as Juliflora oil, methanol, NaOH, measuring cylinders, digital balance, thermometer, heater, and magnetic stirrer were utilized.

2.6.1. Mixing of alcohol and catalyst

Methanol and NaOH were utilized in this investigation since they were less expensive. The catalyst was introduced slowly and carefully while mixing the methanol in a mixer since NaOH catalyst is in solid form and does not quickly dissolve into methanol. According to Refs. [37,38], an ester interacts with an alcohol to produce methyl ester, glycerin, and other contaminants. Three moles of methanol react with 1 mol of triglyceride, NaOH acts as a catalyst in this process. To form a mixture of fatty acid and glycerin esters. The use of 100% biodiesel in an engine is still an issue, although most research suggests that up to 20% biodiesel may be used without any engine modifications [39–44]. 1000 ml juliflora oil was heated to 75 °C in a round bottom flask to drive out moisture and agitated with a magnetic stirrer. The amount of Methanol utilized was 200 ml of 99.9% pure Methanol which is methanol to oil molar ratio of 6:1. In a separate vessel, 40 g (0.6 wt%) of catalyst NaOH with a purity of 99.5% was dissolved in Methanol and put into the round bottom flask of oil while continually stirring the mixture. For 60 min, the mixture was kept at 55 °C and at atmospheric pressure. The mixture was allowed to settle for 8 h under gravity once the *trans*-esterification procedure was completed. Glycerin and juliflora oil methyl ester were the end products of the process. The finished mixture was rapidly churned for half an hour in the mixer at ambient pressure before being allowed to cool at room temperature. Two liquid phases were generated after a successful *trans*-esterification process. Glycerin, excess alcohol, catalyst, contaminants, and residues of unreacted oil make up the bottom layer. Biodiesel, alcohol, and some soap make up the top layer shown in Fig. 5. The biodiesel, alcohol, and some soap in the top layer were separated.

2.6.2. Removal of alcohol

Following the separation of the glycerin and biodiesel phases, the surplus alcohol in each phase was removed using a rotary

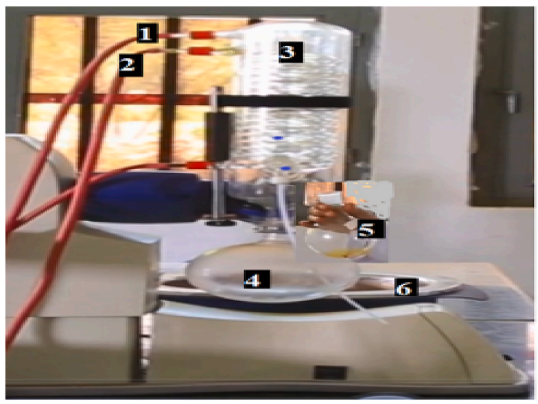

Fig. 4. Rota evaporator (1. Cold water in, 2. Hot water out, 3. Condenser/evaporator, 4. Solvent recovery, 5. Extracted oil, 6. Water bath).

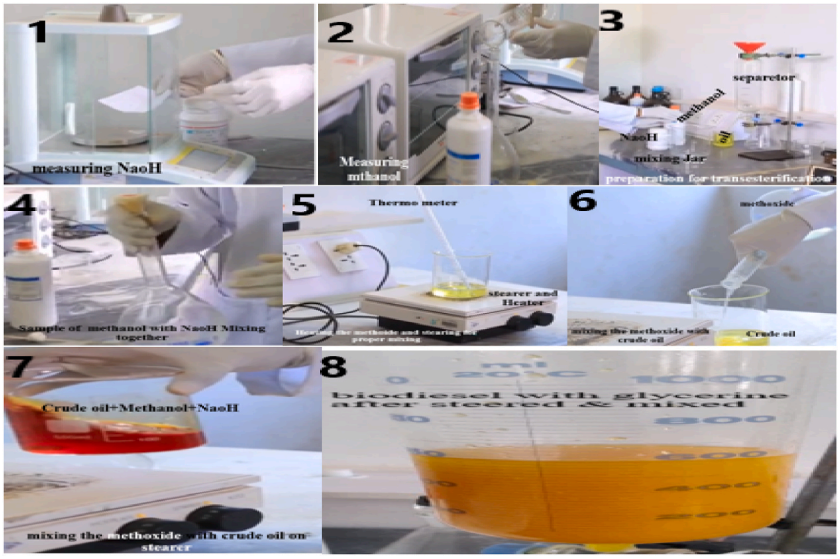

Fig. 5. Transesterification process (1. Measuring NaOH, 2. Measuring CH_3OH, 3. Preparing to mix the methoxide, 4. Mixing the methoxide, 5. Heating and steering the methoxide, 6. Pouring the methoxide on crude oil, 7. Mixing the methoxide with crude oil, 8. The mixture on the gravity separator).

evaporator and a flash evaporation method, as illustrated in Fig. 4.

2.6.3. Methyl ester wash

Water washing, dry washing, and membrane extraction are the three most common methods for purifying biodiesel. Water washing was particularly successful in eliminating both glycerol and alcohol since they were both very soluble in water. It also got rid of any leftover sodium salts and soaps [45,46]. In this investigation, water washing (three times) was employed to wash the contaminants out of the crude biodiesel. The biodiesel was refined after being separated from the glycerin by gently washing it in warm water (heated to 50 °C) to remove any remaining catalyst (NaOH) or soaps, then drying it and storing it. This was often the final stage of the manufacturing process, yielding a clear light brownish liquid with a viscosity close to petro-diesel. The final biodiesel was obtained after washing resulting in 3.9 litters of biodiesel from 6 litters of crude oil. The collection efficiency was above 65% as per eq. (2)

The following formula was used to compute the biodiesel yield:

$$\text{Yield}\ (\%) = \frac{\textbf{litres of biodiesel yield}}{\textbf{litres ofjuliflora oil}} \text{x}100 \tag{2}$$

3. Results and discussion

3.1. Properties of biodiesel and comparison

Biodiesel has properties that are comparable to those of petro-diesel fuel, making it a viable alternative to petro-diesel fuel. The atomic load of triglycerides is reduced to 33% of that of triglycerides when they are *trans*-esterified into methyl or ethyl esters, while the thickness is reduced and the instability is expanded insignificantly. Biodiesel has a similar thickness as diesel fuel. These esters contain 10–11% oxygen by weight, which may enable greater ignition in a motor or engine than hydrocarbon-based diesel fuels. Cetane number of biodiesel is approximately 50, and the addition of tertiary fatty amines and amides improves the start nature of the finished diesel fuel without compromising its primary characteristics. The ignition problem is exacerbated in cold weather because increasing flexibility is difficult. Biodiesel has a reduced volumetric heating quality (approximately 12%), but it has a high cetane number, flash point, cloud point, pour point, viscosity, and consistency [47]. Important properties of different biodiesel as reported earlier are compared to diesel fuel mentioned in table 1 along with that of petro-diesel.

3.2. Characterization of biodiesel

In this paper characterization of Prosopis Juliflora biodiesel was done, concerning density, kinematics viscosity, and calorific value, at Ethiopian petroleum supply Enterprise as per ASTM protocols. The remaining tests were done at Addis Ababa University, Addis Ababa Science and Technology University, and the Ethiopian geological survey authority (see Table 1).

3.2.1. Physico-chemical properties

Prosopis Juliflora has a greater kinematic viscosity than diesel, which is linked to fuel atomization, flow, and distribution. The kinematic viscosity of 3.93 cst implies that the atomization and injection performance will be comparable to diesel, but it also functions as a lubricant for the engine moving components. The biodiesel generated was superior to diesel since it had no Sulphur, whereas diesel contains 0.13% Sulphur [53–55]. As a result, no Sulphur oxides will be generated during the burning of biodiesel, which might harm engine components and have an environmental impact. Similarly, the PJFB generated had no ash content, which might create abrasion on the engine. Table 2, shows comparison of results of JFB from previous studies with current work in this study. The result for the current study of JFB obtained from, bomb calorimeter for calorific value, gravometric capillary for viscosity, hydrometer for density under ASTM standared and detail is shown in Table 3. Cetane number and flash point estimated from the calorific value result and similar estimation also shown in [56].

3.2.2. Testing for pH

The pH electrode was calibrated with a distilled solution before being submerged in the Sample for the pH reading and recording. Based on the recorded test result when compared to diesel 5.6, JFB has a higher PH 9.6 value, and when compared to other biodiesel oils, it has a similar value, showing that the transesterification process was carried out successfully.

3.2.3. Test for copper strip corrosion

This test determines if the copper is susceptible to corrosion. According to Ref. [57]., it is used to determine the degree of copper corrosion that would occur if biodiesel were employed in any application that contains metals like copper [58]. The presence of acids in the biodiesel is monitored by this test. A copper strip blemish test was used to carry out the investigation. In line with ASTM 130 [58], and [57], the obtained result of copper strip corrosion for JFB oil is 1a. Copper strip corrosion has a minimum ASTM standard of 1a and a maximum of 4c. As a result, JFB oil (B100) can be considered as suitable for internal combustion engines.

JFB's pour point and cloud point were 6 °C and 2 °C, respectively, indicating that it has good flow characteristics and may be utilized in cold conditions. The Cetane number of JFB is 68, which is higher than diesel, while for JFB it becomes 52.9 that enables to run the engine more effectively and without difficulty of starting [54]. Because JF has a greater flash point than diesel, it is deemed safe for storage, transportation, and handling. According to ASTM based testing, the FFA percentage of raw JFBO was found to be 0.47, and its biodiesel at 0.14, which lies within the biodiesel standard limit. In Table 3, the thermo-physical and chemical fuel characteristics of JFB oil and diesel were tested and compared for assessment as shown in Table 3.

3.3. Process optimization for biodiesel yield by response surface methodology

The experiments were conducted as per the Box-Behnken response surface design,. Using Minitab 20, the statistical analysis was performed, and analysis of variance was used for experimental optimization (ANOVA). The transesterification process was optimized utilizing a factor of 3 replicates at three levels, necessitating a total of 15 runs and 1 base block. Table 4 includes a list of the researched variable factors, as well as their ranges and levels. The variables were reaction temperature, catalyst load, and methanol to oil ratio. Methanol boiling point, 60 °C, was adopted as the upper temperature level, while the lower limit was 50 °C. Catalyst concentration levels ranged from 0.4% to 2% by weight of oil.

The response variable (biodiesel yield) was used in a full quadratic model once the tests were finished to link the response variable to the independent variable. The entire Box-Behnken experimental design matrix for factorial design is shown in Table 5. To prevent systematic errors, the order in which the runs were made was staggered. The biodiesel production in the transesterification studies ranged from 0.4% to 5.56%, with the maximum content coming from the settings of a 6:1 methanol oil molar ratio, a 2 wt% NaOH catalyst concentration, and a 57 °C reaction temperature.

To forecast JF biodiesel yield % as a function of methanol, catalyst concentration, and reaction temperature, a quadratic regression

Table 1
Important Properties of Different Biodiesels Compared With Diesel Fuel including JFB reported previously, but not for Ethiopian variant juliflora.

Biodiesel feedstocks	Important biodiesel properties					
	Kinematic viscosity @40 °C,in (mm^2/sec)	Density @40 °C, (kg/m^3)	Gross calorific value (MJ/kg)	Flash point (°C)	Cetane number	References
Juliflora	3.25–6.8	887–930	37.6–43.04	181–376	45–49	[19,21,24]
Cotton seed	32.8–36.0	911–921	40.1–40.8	210–243	42–59.5	[48,49]
Karanja	27.8–56	870–928	36–42.1	198–263	45–67	[19,48,49]
Hemp seed	4.72	904	39.1	162	42.7	[19,50]
Mahua	24.6–37.6	891–960	36.8–43.0	212–260	43.5	[19,50,51]
Jojoba curcas	19.2–25.4	863–866	42.7–47.48	61–75	63.5	[48,49]
Linseed	16.2–36.6	865–950	37.5–42.2	108–242	28–35	[19,48,50]
Jatropha	24.5–52.7	901–940	37.2–43	180–280	33.7–52	[38,49,51,52]
Polanga	4–5.34	888.6–910	39.25–41.3	151–170	57.3	[48,52]
Castor	17.14–25	922	38.09–39.5	178.56	37.55–42.3	[38]
Diesel	2.0–3.62	810–840	42–43.8	45–62	45 min	[19,21,24,50]

Table 2
Different literatures' results for JFB were compared to current fuel attributes.

Properties	Present study	Raja.E et al. [20]	Senthil.R et al. [24]	Asokan.M et al. [19]
Density (gm/ml) @15 °C	0.880	0.825	0.832	0.875
Kinematic Viscosity (mm^2/s)@40 °C	3.935	3.246	5.8	6.808
Cetane number	52.9		52	49
Flash point °C	128		113	128
Calorific value MJ/kg	44.4	44.9	43.045	38

Table 3
Comparison of JF biodiesel properties with diesel fuel.

Fuel Properties	Testing methods	Present study	ASTM Limit ASTM D6751	Present study	ASTM Limit ASTM D 975	% deviation of B100 from diesel
		B100	Biodiesel	Diesel	Diesel	
Density@ 15 °C, g/ml	ASTM D4052	0.8941	0.880	0.8387	848	6.2
Density@ 20 °C g/ml	ASTM D4052	0.8907	–	0.8353	–	6.2
Kinematic Viscosity @ 40 °C (cSt)	ASTM D445	3.9354	1.9–6.0	3.0353	1.3–4.1	22.87
Gross Calorific value (MJ/kg)	ASTM D240	44.4	–	44	42.52	4.23
Cetane number	ASTM D976	52.9	47 min	49	40–55	7.37
Flash pint °C	ASTM D93	128	100–170	75	60–80	41.4
Specific gravity@ (27 °C)	ASTM D1298	0.8568	–	0.8234	–	3.898
Saponification value (mgKOH/g)	ASTM D5558	163.6	370 max	–	–	–
Iodine number (gI_2/100 g)	EN,14,111	99.8	120 max	–	–	–
Pour point (°C)	ASTM D97	6	−15 to 16	−12	−35 to −15	–
Cloud point (°C)	ASTM D2500	4	−3 to 12	−7	−15 to 5	–
Copper strip corrosion test	ASTM D130	1a	4c max.	1a	4c max.	Same
Acid number (mg KOH/g)	ASTM D664	0.28	0.5 max	–	–	–
Total glycerin (%mass)	ASTM D 6548	0.04	<0.24	–	–	–
PH value@ (22 °C)	–	9.6	–	5.6	–	41.6
Water and sediment (%) PPM	ASTM D2709	0.02	0.05 vol %	–	161	–
Fuel composition	ASTM D6751	C16-22 FAME	C12-22 FAME	–	C10-21 HC	–
FFA (%)	–	0.14	–	–	–	–
Methyl ester content (%)		99.8	>96.5	–	–	–

Table 4
Coded variables and experimental levels of ANOVA parametric optimization used in RSM.

Factors	Unit	Coded symbol	Range and levels		
			Low (−1)	Medium (0)	High (1)
Methanol to oil ratio	ml	A	60	80	120
NaOH catalyst	wt%	B	0.4	1.5	2
Temperature	°C	C	50	55	60

model with specified coefficients for statistical prediction as defined by eq. (3) was created using Minitab 20 based on the coded parameters. The calculated F-values, consequent regression coefficients, and accompanying P-values are listed in Table 6.

3.4. Analysis of variance (ANOVA)

Analysis of variance (ANOVA) was employed for optimization of the JFB yield and results are shown Table 6. The main effects (A, B and C) get linearly represented and statistically significant except B(NaOH) and C (temperature) whereas the quadratic effects of (A^2, B^2) and from the interactive effects AB, BC are significant.

$$\text{Biodiesel (\% yield)} = 5.6 + 0.5137\,A - 5.67\,B + 0.764C + 0.002242\,A \times A + 1.752\,B*B - 0.00641C \times C + 0.09460\,A \times B + 0.000472\,B*C - 0.1206\,B \times C \quad (3)$$

Where, = A-Methnol (ml), B–NaOH (wt%), C- reaction temperature (°C).

To assess the statistical significance and fitness of the model equation, analysis of variance (ANOVA) was used. The chosen response's impact on significant individual variable and their relationship was also examined by ANOVA. Table 7 displays these outcomes. Due to the greater F value (39.96) and lower P value (0.0001), the results demonstrate that the model is highly significant at the 95% confidence level. When evaluating the significance of each regression coefficient, the P value, which expresses the chance of error,

Table 5
Result and experimental matrix for Box-Behinken design.

StdOrder	RunOrder	PtType	Blocks	A (ml)	B (wt%)	C (°C)	Biodiesel Yield (%)		
							Experimental	Prediction	Residual
6	1	2	1	113	1.2	50	2.43	2.341696	0.088304
5	2	2	1	60	1.2	50	1.59	1.741491	−0.15149
1	3	2	1	60	0.85	55	2.62	2.678439	−0.05844
14	4	0	1	86.5	1.2	55	0.41	0.402124	0.007876
12	5	2	1	86.5	2	60	0.52	0.7194	−0.1994
15	6	0	1	86.5	1.2	55	0.41	0.402124	0.007876
7	7	2	1	60	1.2	60	1.09	1.166491	−0.07649
13	8	0	1	86.5	1.2	55	0.41	0.402124	0.007876
4	9	2	1	113	2	55	5.56	5.52981	0.03019
9	10	2	1	86.5	0.4	50	1.23	1.042413	0.187587
2	11	2	1	113	0.4	55	1.11	1.391798	−0.2818
10	12	2	1	86.5	2	50	2.01	2.1344	−0.1244
11	13	2	1	86.5	0.4	60	1.67	1.557413	0.112587
8	14	2	1	113	1.2	60	2.18	2.016696	0.163304
3	15	2	1	60	2	55	1.08	0.79358	0.28642

Table 6
Analysis of variance for the experimental results of the Box-Behinken design matrix for JFB yield.

Source	DF	Adj SS	Adj MS	F-Value	P-Value	remarks
Model	9	23.9034	2.6559	39.96	0.000	Highly significant
Linear	3	1.3910	0.4637	6.98	0.031	Significant
Methanol	1	0.9853	0.9853	14.82	0.012	Highly significant
NaOH	1	0.0263	0.0263	0.40	0.557	Not significant
Temperature (°C)	1	0.4050	0.4050	6.09	0.057	Not significant
Square	3	10.6944	3.5648	53.63	0.000	Highlysignificant
Methanol × Methanol	1	8.7170	8.7170	131.15	0.000	Highly significant
NaOH × NaOH	1	3.8555	3.8555	58.01	0.001	Highly significant
Temperature (°C) × Temperature (°C)	1	0.0937	0.0937	1.41	0.288	Not significant
2-Way Interaction	3	12.0229	4.0076	60.30	0.000	Highly significant
Methanol × NaOH	1	11.0760	11.0760	166.64	0.000	Highly significant
Methanol × Temperature (°C)	1	0.0156	0.0156	0.24	0.648	Not significant
NaOH × Temperature (°C)	1	0.9312	0.9312	14.01	0.013	Highly significant
Error	5	0.3323	0.0665			
Lack-of-Fit	3	0.3323	0.1108	*	*	
Pure Error	2	0.0000	0.0000			
Total	14	24.2358				

Regression analysis was undertaken for fitting the response function and predicting the biodiesel yield was obtained in eq. (3).

Table 7
Coded regression Coefficients of predicted quadratic polynomial model.

Term	Coef	SE Coef	T-Value	P-Value	VIF
Constant	0.402	0.147	2.74	0.041	
A	0.3626	0.0942	3.85	0.012	1.07
B	0.063	0.101	0.63	0.557	1.10
C	−0.2250	0.0911	−2.47	0.057	1.00
A × A	1.575	0.137	11.45	0.000	1.06
B × B	1.121	0.147	7.62	0.001	1.17
C × C	−0.160	0.135	−1.19	0.288	1.02
A × B	2.006	0.155	12.91	0.000	1.15
A × C	0.062	0.129	0.48	0.648	1.00
B × C	−0.483	0.129	−3.74	0.013	1.00

is utilized. The P value also reveals how each cross product interacts with the others. A big F value resulting from noise has a 0.01% chance of occurring, according to the P value of.0001. In this instance, the generation of biodiesel is significantly influenced by A (methanol ratio), C (reaction temperature), A^2 (quadratic effect of methanol amount), B^2 (quadratic effect of catalyst concentration), and AB (methanol quantity with catalyst). Due to its larger F value (131.15) and lower P value (0.0001), methanol (A) is the most significant variable in the production of biodiesel from JFB. The yield of JFB biodiesel is negatively impacted by catalyst concentration (C), as shown by regression model eq. (3). The speed of the transesterification reaction will therefore be slowed by increasing both the catalyst concentration and temperature. The model's "Lack of Fit" shows that the link between the independent variables (M, C, and T)

and the dependent variable is not well described (JFB Biodiesel yield). In this investigation, the related lack of fit becomes minor, showing that the quadratic model and the experimental data fit well together. The coefficient of determination served as proof of the model's fitness quality (R^2). The adjusted coefficient of determination (Adj. R^2) was 96.16% whereas the coefficient of determination (R^2) was 98.63%. The calculated coefficient value shows that the model is fairly accurate. For experimental relationships between the variables and the response, the model is, in conclusion, extremely suitable. The comparison of experimental and anticipated biodiesel yields in Fig. 9a illustrates how accurate the prediction model is. All points are in close proximity to the straight line, indicating that the experimental and anticipated values coincide well.

3.5. Response surface plots for JF biodiesel production

Plotting three-dimensional surface curves against any two independent variables, while maintaining other variables at their central level, allowed one to examine the influence of the process factors on the transesterification efficiency. Figs. 6–8 display the surface plots and contour plots of the yield determined by eq. (3). To comprehend how the variables interact and to establish the ideal value of each variable for the greatest response, the response surface curves were plotted on Fig. 9a–c.

3.5.1. Effect of methanol and catalyst concentration on JFB yield

Fig. 6 displays the 3D response surface and 2D contour plot between methanol and NaOH catalyst concentration for various fixed parameters (reaction temperature 55 °C and time 60 min). The greatest amount of catalyst concentration results in a biodiesel yield (%) of 113 ml with an increase in Methanol weight percentage. At NaOH of 2 wt%, the highest JFO methyl ester was discovered to be 5.56%. When the catalyst concentration is lower (1.2 wt%) and the methanol concentration stays constant at 113 ml, as shown by the Box-Behnken experimental matrix in Table 5, the JFO methyl ester drops to 2.43% at 50 °C. Once more, at 113 ml of methanol, catalyst concentrations of 0.4 and 1.2 wt%, and a mean temperature of 55 and 60 °C, the yiel drops to 1.11 and 2.18%. Hence, although high catalyst concentrations might result in phase separation and emulsion, catalyst concentration is one of the key elements in increasing biodiesel yield [60]. According to Table 6 's ANOVA results, the interaction between the concentration of the NaOH catalyst and the methanol was found to be less significant.

3.5.2. Effect of catalyst concentration and temperature on JFB yield

The 3D surface plots and 2D contour plots in Fig. 7 illustrate how the concentration of the catalyst and the reaction temperature affect the biodiesel yield. A rise in reaction temperature (50 °C) and a mid-level concentration of NaOH catalyst (1.2 wt%) can boost

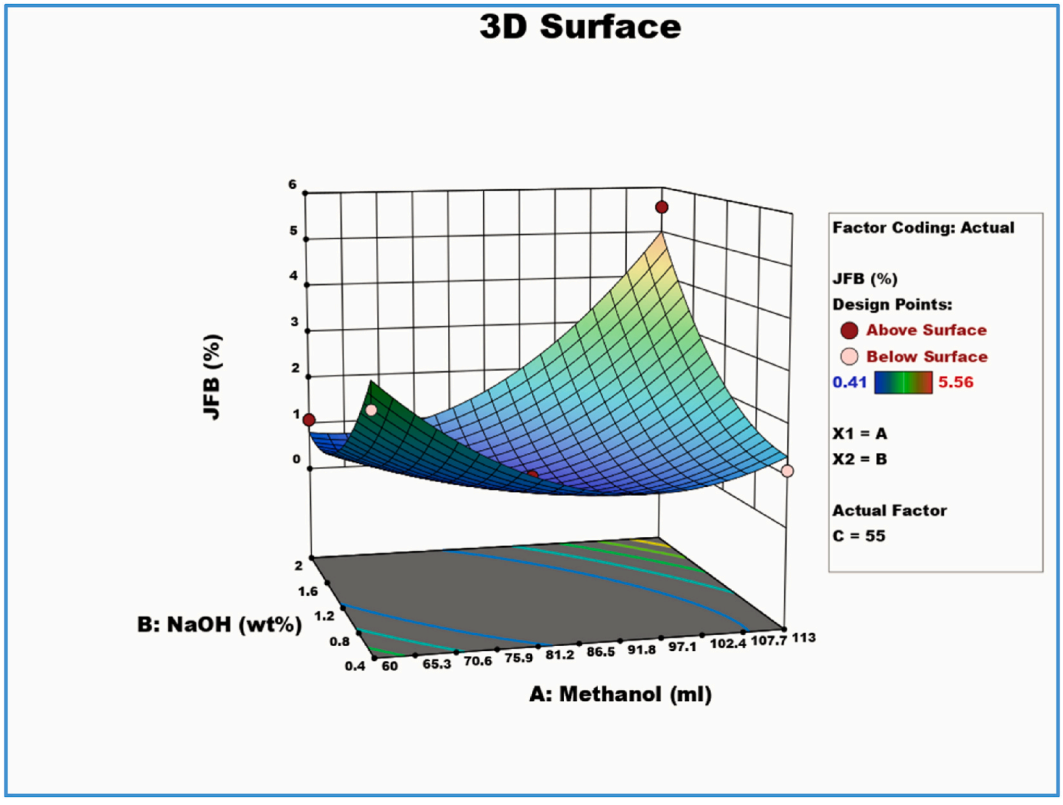

Fig. 6. 2D Response contour plot and 3D response surface plot for combined effects of methanol (A) and catalyst (B).

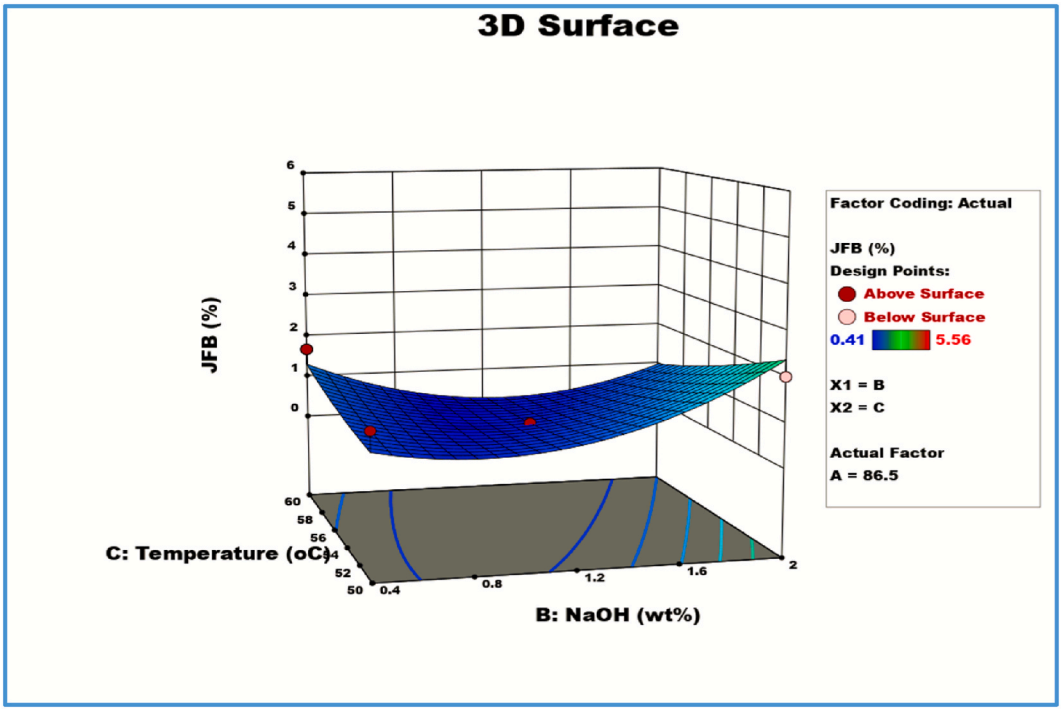

Fig. 7. 2D Response contour plot and 3D response surface plot for combined effects of catalyst (B) and temperature (C).

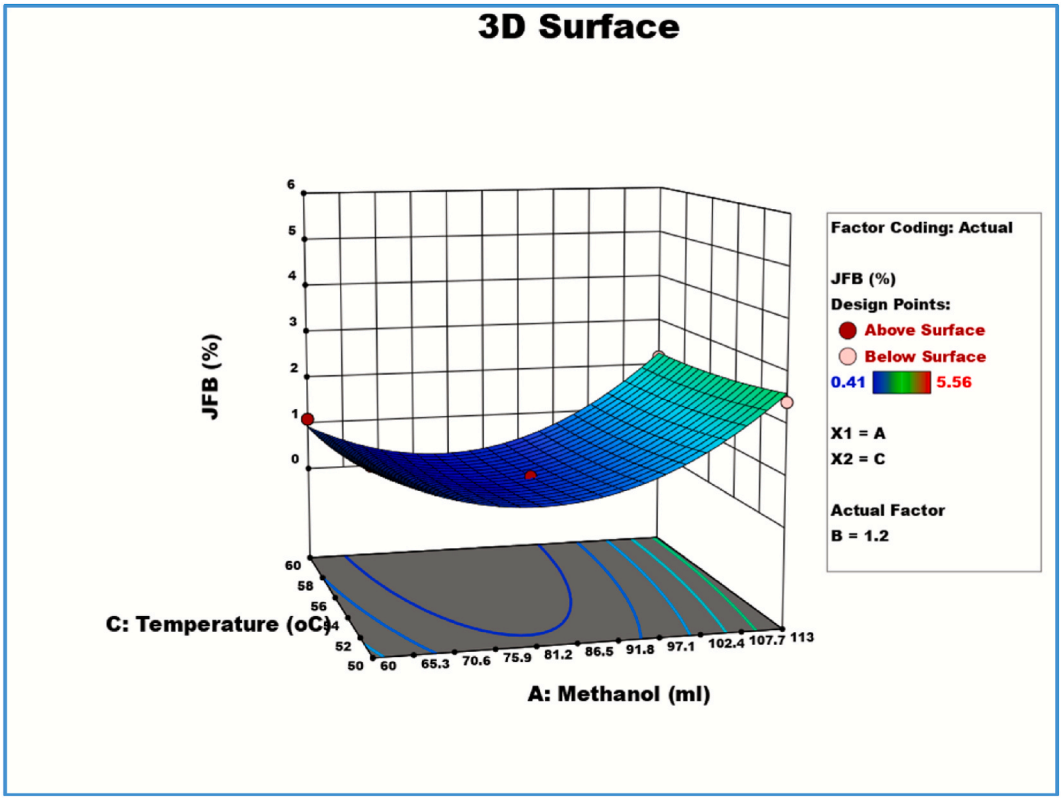

Fig. 8. 2D Response contour plot and 3D response surface plot for methanol (A) and temperature (C) on the biodiesel yield.

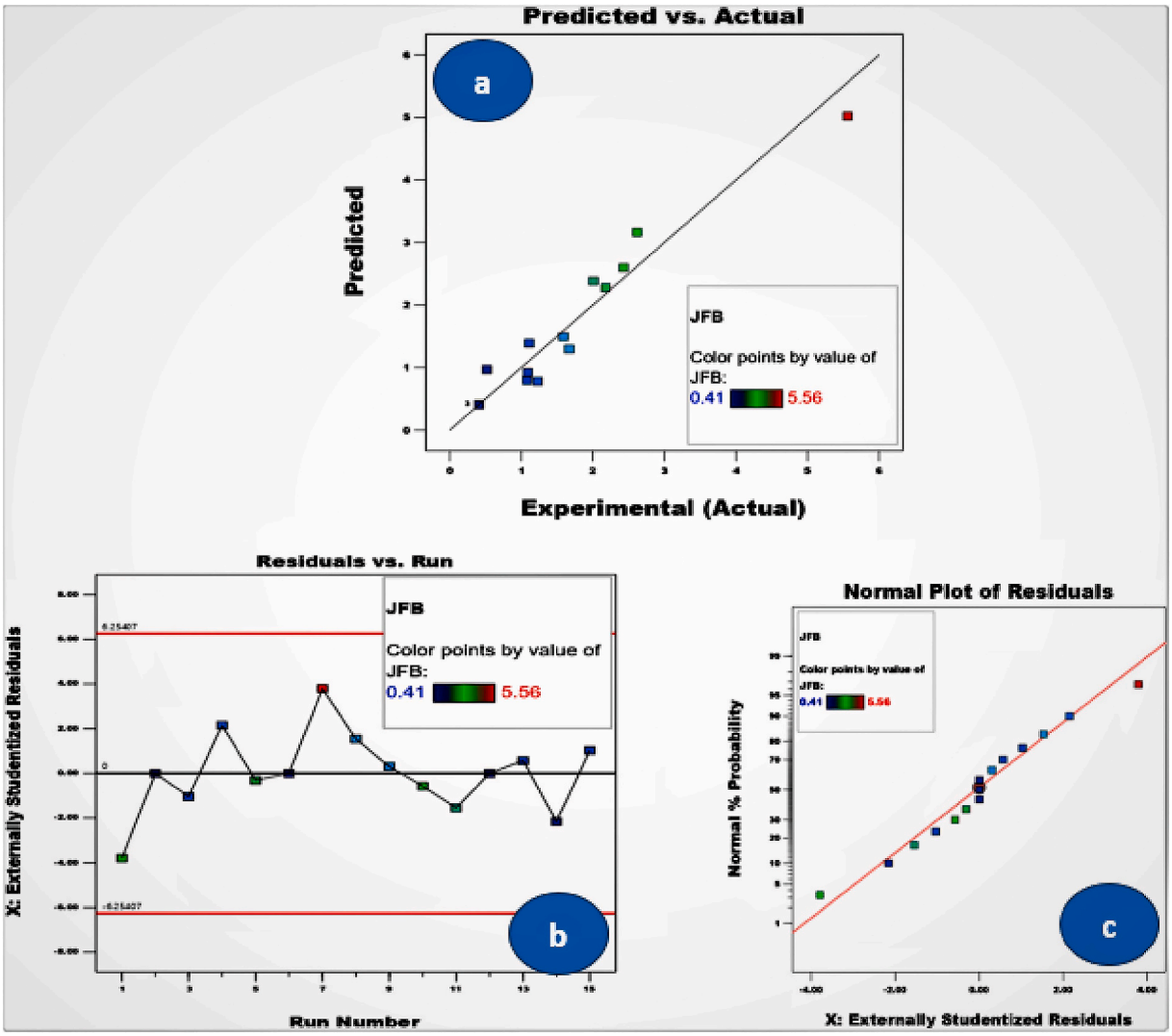

Fig. 9. Diagnostic plots for (a) plot for compare the actual and experimental yield, (b) plot for residual vs run, (c) plot for externally studenized residuals.

the biodiesel production by up to 1.59% while maintaining the variables of Methanol concentration and reaction time of 60 min. The yield of biodiesel decreased to 1.08% when the reaction temperature was raised to 55 °C and the catalyst concentration was increased to 2 wt%. Similar results were obtained by increasing temperature from (50, 55, and 60 °C) and lowering catalyst concentration to the lower level (0.4 wt%), which decreased biodiesel output to 1.23, 1.11, and 1.67% while maintaining methanol at 86.5 ml as a constant. The generation of soap may be strongly impacted by the high temperature and catalyst concentration, which may favor the saponification of triglycerides and lead to decreased biodiesel yield [61]. There is no statistically significant interaction between the concentration of NaOH catalyst and reaction temperature, as can be seen from Table 6 ANOVA results.

3.5.3. Effect of temperature and methanol on JFB yield

Fig. 8 illustrates how a rise in reaction temperature reduces the production of biodiesel. Increased temperatures (over 55 °C) slowed down the transesterification process, which led to a lower yield of biodiesel. The molar ratio of methanol to oil was also crucial in raising the biodiesel output. It was discovered that 113 ml of methanol was the ideal amount, and that lowering the methanol (below 113) reduced the production of biodiesel. The maximum biodiesel yield was achieved at a reaction temperature of 55 °C (5.56%) with an increased concentration of (113 ml). When the process temperature was raised from 50 °C to 60 °C, the overall biodiesel yield drastically reduced (2.43–2.18%). The evaporation of methanol at 65 °C is the primary cause of the reduced biodiesel production [12]. So, it can be infered that an important aspect of the generation of biodiesel is the reaction temperature. It was determined that a temperature of 55 °C was ideal for reactions. The relationship between the reaction temperature and the amount of methanol was determined to be significant based on the ANOVA results in Table 6. The greatest F-values in the ANOVA findings showed that

methanol was the process variable that had the biggest impact on JFO biodiesel yield (Table 6). The ideal conditions are 55 °C for the reaction, 2 wt% NaOH Catalyst, and 113 ml of methanol, or a 6:1 M ratio. The ideal biodiesel production was estimated to be 96.48%. Experiments were conducted under these ideal conditions to validate the projected optimal values, and the observed values (5.56%) nearly matches with the expected value (5.52%) from the regression model.

3.5.4. Diagnostic plots

Additional plots were utilized to assess the model's suitability and determine whether the model equation would produce accurate approximations of the real value. Moreover, Fig. 9a demonstrates the close correspondence between the anticipated values and the experimental results. These also show how the model may be used to forecast the ideal circumstances for the transesterification process's highest possible biodiesel yield. The externally studentized residuals plot (Fig. 9b) was created to represent the model's fitness and demonstrate that all the data points lie within the limits of (±2). The normal% probability plot of residuals for biodiesel production is continuously distributed, as shown in Fig. 9c, and the data are close to a straight line indicating that the variance is not out of the ordinary.

3.6. Effect of agitation time on crude oil extraction yield

The maceration or breaking up of the oil from the hard powder seedpod was done using each separate container by increasing agitation time Maceration is a remedy prepared by soaking plant material in vegetable oil, chemical, or water to separate oils in it from the plant material [62]. The process of maceration makes the material soft. During the experiment, the effects of mixing time duration on oil yield with the help of hexane solvent were investigated. Two kilograms of crushed seedpod equally prepared for each 6 block separate containers with a solvent mixture of 2.5 litters hexane. To see the effects of maceration time on mixed solutions to extract oil from it, six separate containers of the different batches were prepared as shown in Fig. 3, number 1. Each container has 2.5 litters of hexane solvent with 2 kg of crushed seedpod for maceration based on the standard laboratory procedure indicated in Ref. [63].

For each batch, different maceration periods were given to observe the effect of mixing and agitation time on crude oil yield, which is from one-half a day up to five days duration. Agitation time was varied on the magnetic stirrer with constant speed of 300-rpm based on the standard mixing and agitation time. Therefore, three days duration is the optimal period in which the highest yield would be possible to obtain as pointed out, [63]. As shown in Fig. 10, with the maceration time increasing, the crude oil yield increases at an increasing rate but after three days the oil yield is nearly the same or steady. This means most of the oil is macerated up within three days' time interval i.e. three days is the optimal period for the oil extraction process. The macerated solution obtained is hexane and crude oil. Further separation of the solvent from crude oil is done on a soxhlet extractor in combination with the Rota evaporator. Finally, from the optimum solution of hexane with crude oil, 1.5 litters of hexane were recovered and 0.5 litters of crude oil were obtained from the 2-kg crushed seedpod. Therefore, 90% of oil is prepared from the batch extraction process; even though batch oil extraction provides much oil yield it needs more agitation time and mixing period. Further increase of mixing time may not increase the recovery of the oil due to the stability of equilibrium and saturation of solvent with the solute. From these batches, oil obtained in one single batch was 480 ml and with total oil obtained from all batches amounting to 5 L.

3.7. Effect of reaction time on biodiesel oil extraction

The influence of mixing time was investigated and shown in Fig. 11. To enhance the conversion of triglycerides, reaction time is highly crucial. Because oil and solvent are not entirely miscible when the transesterification reaction begins, the reaction occurs on the catalyst's surface. However, as the reaction time rises, the solubility of oil and methanol increases, increasing the total yield of biodiesel synthesis by heating the mixture to 50 °C while keeping all other variables constant. All of the blocks were made of 8 g of sodium hydroxide, 400 mL of methanol, and 200 mL of crude JFB (molar ratio of 6:1 for methanol to oil ratio common to all the blocks). Within

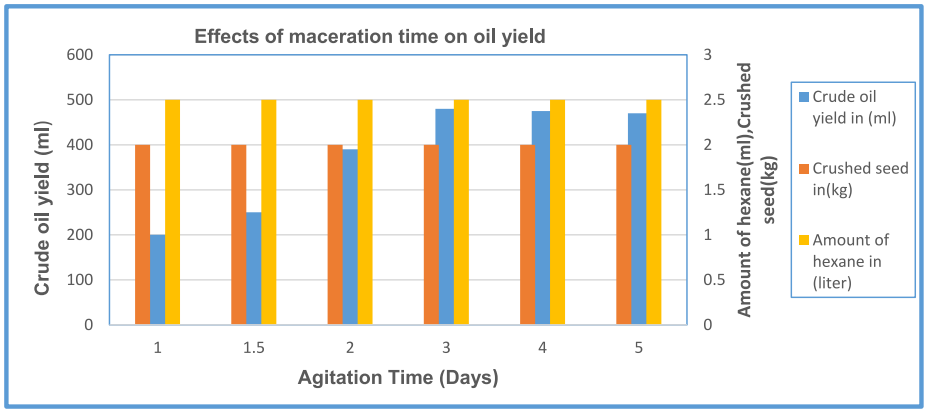

Fig. 10. Effect of agitation time on crude oil yield.

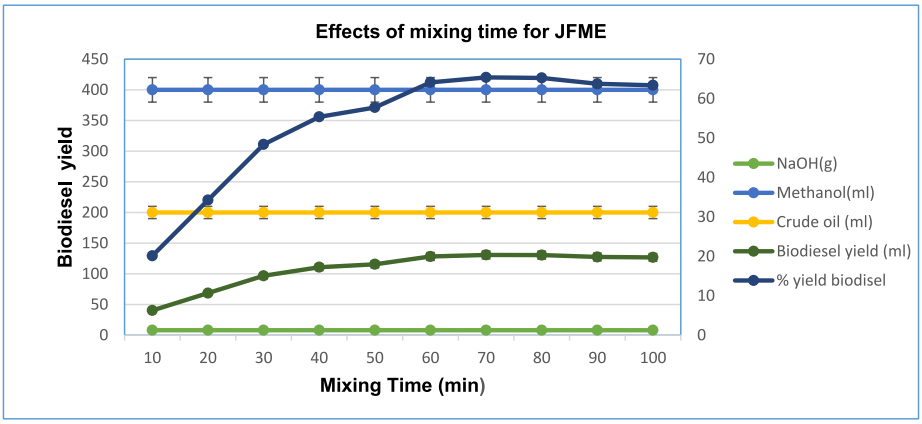

Fig. 11. Effects of mixing time on JFME oil recovery.

this mixed ratio, a 10-min time gap was maintained from 0 to 70 min mixing time. There are ten blocks filled with solvents combined with JFB. The volume of crude oil and solvents were the same, but the mixing duration was varied. Then a 40 ml oil extracted from the first block was maintained for 10 min of mixing time. However, when the mixing time was prolonged, the rate of oil yield increment rose as well, reaching a high of 130 ml at 70 min, which is 65% of the crude oil at the same 50 °C temperature for all the blocks. The % difference between extracted oil with a 10 min and a 70 min mixing time was 45%, indicating that as the mixing time rises, the oil output increases as well, resulting in an increase in biodiesel yield. The concentration of fatty acid methyl esters did not go up as the reaction time was increased further. This might be due to the formation of equilibrium between reactants and products [59]. At this point, all available energy was being used to create the transesterification equilibrium that gave the best results. After 80 min, there was a drop in biodiesel output, and then the equilibrium level was attained. This may be explained by the fact that increasing the reaction time causes the reactants and products to hydrolyze, boosting soap production. Similar effects are also shown under different biodiesel studies [64,65].

3.8. *FT-IR analysis of prosopis juliflora biodiesel*

To discover and investigate the mechanisms of the functional groups required for the biodiesel, the functional groups discovered in JFB pure biodiesel (B100) and pure diesel (D100) samples were compared and appraised to see if they are within the range of biodiesel requirements or not. Biodiesel and diesel include a variety of functional groups. The main factors are important functional group materials. Pure biodiesel and pure petro diesel were prepared in the form of droplets with spectroscopic grade KBr to validate the

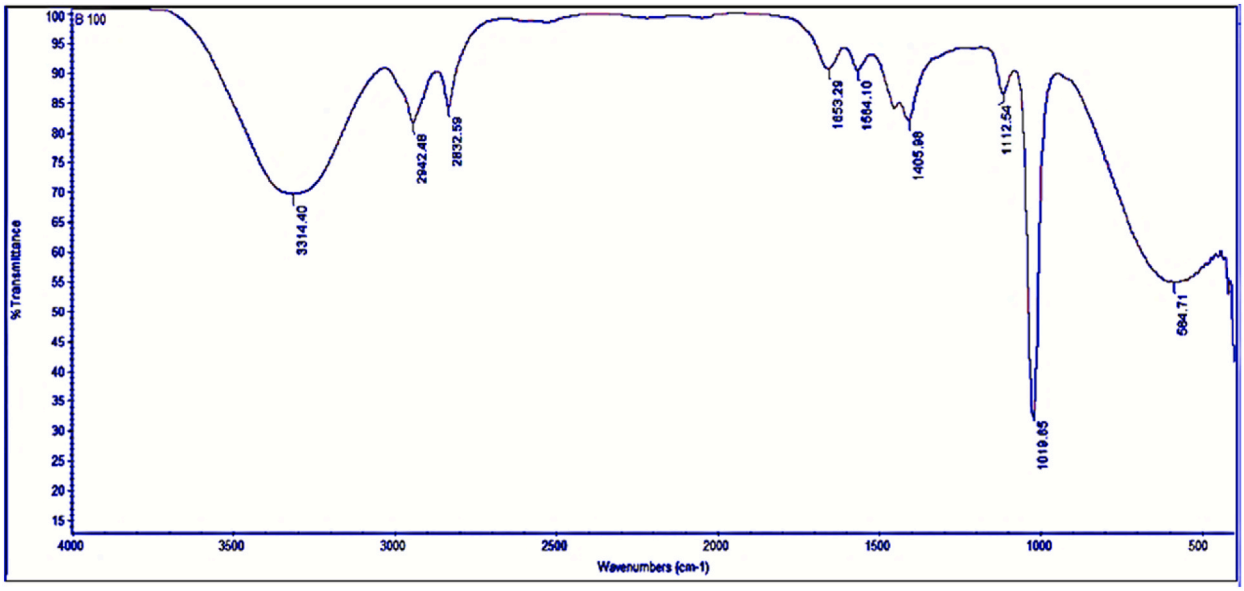

Fig. 12. The spectra of FT-IR analysis for B100.

functional groups involved in biodiesel and its mixes in the present wave numbers with transmittance. Droplets of the sample were generated and scanned in the spectral range of 4000–500 cm^1.

3.8.1. FT-IR analysis for JFB (B100)

Fig. 12, displays the FT-IR spectra for pure biodiesel, which reveals a variety of distinct functional group peaks, showing the complex nature of functional groups accessible on biodiesel samples. The vibration bands of the biodiesel are owing to the presence of hydrogen-bonded OH stretch (alcohol) at 3314.40 cm^{-1}, methyl C–H stretching at 2942.48 cm^{-1}, and methylene C–H stretching at 2832.59 cm^{-1}, as shown in the FT–IR spectra. Furthermore, among the biodiesel functional group alkenes, ester was discovered at a peak of 1653.29, 1112.54, and 1019.65 cm^{-1}, respectively, and is attributable to C=C and C–O functionalities. The major biodiesel peaks of the functional groups, including the fingerprint region, have changed for their functional group's band intensities and frequencies after biodiesel uptake, as shown in Table 8 and Fig. 19. This confirms the methyl ester participation of these functional groups in the biodiesel (B100). But, previous investigations [11], exhibit different FTIR spectra peaks and stretching points than the current investigations of the identical JFB presented and the result confirmed the existence of phenols, alcohols, and water at peaks of 3200–3400 $cm^{-1}$and 900–1300 cm^{-1}, alkenes and aromatics at peaks of 1575–1675 cm^{-1}, and monocyclic and aromatic groups at peaks of 1420–1610 cm^{-1}. However, in the current investigations these functional groups were present at a different wave length positions and this might be on account of the site and soil specific JF feedstock variations and extraction techniques for JFB.

The FT-IR analysis for B100 shows the different functional groups that existed on biodiesel concerning wavelength (cm^{-1}) and transmittance as a percentage peak value interpreted in Table 8, that the methyl ester group necessary for biodiesel were available.

3.8.2. Chemical composition of biodiesel

Oils from diverse sources have varied unsaturated fatty compositions from a synthetic standpoint. The length of the unsaturated fatty acid carbon chain and the number of unsaturated links it contains vary. Fats and oils are made up of 1 mol of glycerol and 3 mol of unsaturated fats and are generally water-insoluble, hydrophobic compounds found in plants. These are commonly referred to as triglycerides. Because completely saturated triglycerides are strong at room temperature and so can't be used as fuel, they contribute to excessive carbon storage in motors and engines. The unsaturated fatty acids differ in chain length, unsaturation level, and proximity to other substance capabilities. Palmitic, oleic, and linoleic unsaturated fats are more prevalent in the alkyl chain of triglycerides in edible and non-edible oils and are classified and identified by their unsaturated fatty acid content. Palmitic, arachidic, behenic, lignoceric, oleic, erucic, linoleic, and other fatty acids are found in varying amounts in these oils. Table 8. Shows the empirical formula and structure of several common fatty acids of saturated and unsaturated fats found in edible and inedible oils. Triglyceride particles have molecular weights between 800 and 900, making them nearly multiple times larger than standard diesel ($C_{16}H_{34}$) fuel. Edible and non-edible oils have lower volatility due to their larger molecular weight, while edible and non-edible oils are fundamentally more sensitive than diesel due to their unsaturation. As a result, they are much more vulnerable to oxidation and heat polymerization reactions.

The fatty acid compositions obtained from the present study, as shown in Table 9, were the most important and frequently existing fatty acids in different biodiesels and it's within the list of common fatty acid compositions from different biodiesel structures. The detailed fatty acid compositions obtained from the present study were shown in Table 10.

3.9. The GC-MS analysis result for prosopis juliflora biodiesel (B100)

Several chemicals were identified as a consequence of the GC–MS analysis of the JFB (B100) extract. Mass spectrometry coupled with gas chromatography was used to identify these chemicals. Table 10 lists the different chemicals identified by GC–MS in the extract. Fig. 13, shows a fatty acid chromatogram that depicts the various components found in JFB FAME (Juliflora biodiesel Fatty acid methyl ester)[67]. The saturated fatty acids in Julyflora biodiesel were 98–99%, which is lower, while the unsaturated fatty acids were relatively higher. As a result, greater JFB methyl ester was detected in unsaturated fatty acids. As is known, the content of fatty acids reflects the quality of the fuel. Greater saturated fatty acid content improves oxidation stability but lowers cloud point and pour point of biodiesel, whereas higher unsaturated fatty acid content improves cloud point but has poor oxidative stability [68,80]. Fig. 13 shows the mass spectra of all the chemicals found in JF biodiesel. The most prevalent chemicals were found on first peak Docosenoic acid methyl ester, (Z-), second peak Hexadecanoic acid methyl ester, third peak Octadecenoic acid methyl ester,(Z)-, fourth peak

Table 8
FT-IR spectrum analysis for B100.

Wave number (cm^{-1})	Positions of infra-red bands	Functional group	Relative positions
3314.40	Unsaturated hydrocarbon Amine (*N*–H) group and alcohol (O–H)	C–N Amine C–O–H	Far
2942.48 2832.59	Aliphatic methyl C–H stretching and methylene C–H stretch Group	CH-3-,-CH2-	Far
1653.29	Unsaturated Alkenes C=C, C–O Amide, Vinyl, Vinylidene, Cis	fx1	Middle
1564.10	No effect	No effect	Middle
1405.98	No effect	No effect	Near/Finger print
1112.54	Oxygen (C–O) group, Ester	C–O–C	Near/Fingerprint
1019.65	Unsaturated Alkenes and Ether	C=C and C–C	Near/Fingerprint
584.71	No effect	No effect	Near/Fingerprint

Table 9
Common fatty acid compositions of biodiesel.

Fatty acid names	Formula	Structure	References	Present studies
Palmitic	$C_{16}H_{32}O_2$	16:0	[55,59]	Palmitic
Stearic	$C_{18}H_{36}O_2$	18:0	[22,60]	
Myrestic	$C_{14}H_{28}O_2$	14:0	[62,69,70]	
Lauric	$C_{12}H_{24}O_2$	12:0	[66,71]	
Arachidic	$C_{20}H_{40}O_2$	20:0	[72,73]	
Linolenic	$C_{18}H_{30}O_2$	18:3	[66,69]	Linolenic
Linoleic	$C_{18}H_{32}O_2$	18:2	[66,74]	Linoleic
Oleic	$C_{18}H_{34}O_2$	18:1	[66,75]	Oleic
Behenic	$C_{22}H_{44}O_2$	22:0	[66,76]	
Lignoceric	$C_{24}H_{48}O_2$	24.0	[66,77]	
Erucic	$C_{22}H_{42}O_2$	22:1	[64–66]	Erucic

Table 10
GCMS identification of compounds compositions for JFB (B100).

PK#	RT	Area Pct	Compound name (library ID)	Molecular formula	Molecular Weight	Compound nature	Ref #	CAS no.	Qual.
1	7.7597	68.8148	13-Docosenoic acid, methyl ester, (Z)-	$C_{22}H_{44}O_2$	340.58	Eurcic Acid	207,458	001120-34-9	99
2	11.4261	2.0836	Hexadecanoic acid, methyl ester	$C_{16}H_{32}O_2$	256.43	Palmitic acid	130,813	000112-39-0	98
3	13.2925	4.1595	6-Octadecenoic acid, methyl ester, (Z)-	$C_{18}H_{36}O_2$	282.45	Oleic acid	155,752	002777-58-4	99
4	13.3568	5.7749	9,12-Octadecadienoic acid (*Z,Z*)-, methyl ester	$C_{18}H_{32}O2$	280.44	Linoleic acid	153,890	000112-63-0	99
5	13.5568	19.1672	9,12,15-Octadecatrienoic acid, methyl ester, (*Z,Z,Z*)-	$C_{18}H_{30}O2$	278.42	Linolenic acid	152,040	000301-00-8	99

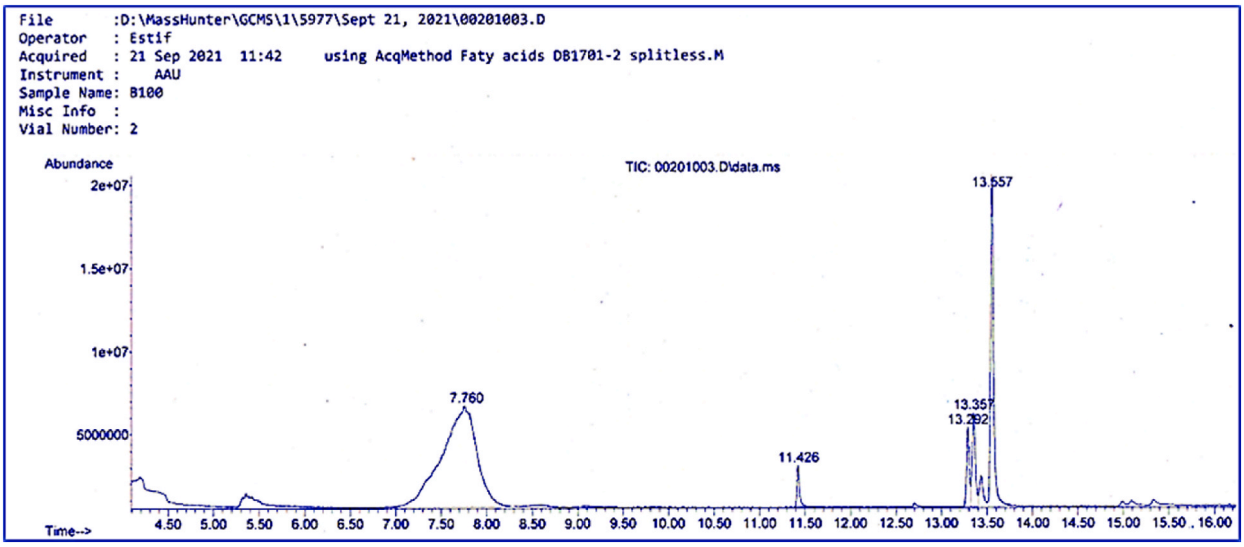

Fig. 13. GCMS fatty acid composition result for JFB (B100).

Octadecadienoic acid methyl ester, (ZZ)-, and fifth peak Octadecatrienoic acid methyl ester, (ZZZ)-. Docosenoic acid methyl ester (Z-), with a peak retention time of 7.7597 and a molecular weight of 352.6 g/mol, was published with a CAS number of 1120–34-9 and a molecular weight of 352.6 g/mol. Other compounds were discovered and reported in the same way.

Methyl palmitoleate, methyl linoleate, methyl palmitate, methyl behenate, and methyl oleate are most likely the five components isolated by GC. It indicates that palmitic acid, palmitoleic acid, oleic acid, linoleic acid, and Eurcic acid are the main fatty acids found in the methyl ester of Julifora oil. The various esters are calculated using the standard database and the retention period mentioned above each compound's peak. The fatty acid content of Julifora biodiesel was determined using GC-MS techniques. Gas chromatography analysis is used to evaluate the fatty acid content of Julia methyl ester. Table 10 shows the chromatogram of a Julifora methyl

ester sample. Erucic acid (68.81%) has the greatest unsaturated fatty acid concentration, followed by linoleic acid (19.16% and linolenic acid at 5.77%. The saturated fatty acid compositions of single bond oleic acid at 4.15 and Palmitic acid (2.08) were exhibited as a saturated fatty acid. The amount of total saturated and unsaturated fatty acids in Julifora methyl ester is 93.03% and 6.97%, respectively. Comparable to studies reported earlier [24].

3.9.1. Analysis of fatty acid composition

Table 10 depicts the main fatty acids found in Julifora biodiesel. The fatty acid composition of vegetable oils varies depending on the nature and kind of feedstock. The most often reported compositions are stearic, palmitic, oleic, linoleic, and linolenic acids. The biodiesel made from Juliflora has a larger proportion of unsaturated fatty esters than saturated fatty esters. Two significant components of JFME are methyl esters of linoleic acid and palmitic acid, as can be inferred from the data. The first compound's absorption spectra are unsaturated, whereas the second is saturated. The fatty acid, linoleic acid is found in greater amounts as one of the primary fatty esters in the JFME composition in this research. In the present study a new fatty acid was observed in his study exceptionally as eurcic acid with a value of 68.81 compared to the previous studies on JFB. The methyl esters were purified and included FAME, with carbon chain lengths primarily ranging from C_{14} to C_{18}, indicating that they are an appropriate biodiesel fuel. According to a previous study [34]. The JFB in present study has carbon chain lengths primarily ranging from C_{14} to C_{22}, indicating that they are an ideal biodiesel fuel. The current studies of JFB carbon chain lengths were from C_{16} to C_{22} which is within the range of ideal biodiesel. The presence of various organic compounds as estimated from FT-IR already presented the preceding section, were in agreement with GC-MS findings.

3.10. ^{1}H NMR and ^{13}C NMR analysis of compounds' structural properties in the JFB-oil

In Fig. 14 the ^{1}H NMR analysis of JFB is displayed. The spectra can be divided into three primary groups based on chemical shifts caused by different proton types: aliphatic, olefin, and aromatic. More than 55% (mass) of the molecules in this spectrum are aliphatic. In the chemical shift range of 0.0–2.5 ppm, aliphatic resonances take place. The protons connected to the carbon atoms of alcohols, esters, and ethers (H–C–OH, HCOR, RCOO-C-H) are represented by the next region of 2.5–5.0 ppm [21,26]. Protons bound to heteroaromatics are indicated in the range from 6.0 to 8.6 ppm, and aldehydes are present in the region from 8.6 to 9.0 ppm.

Fig. 15 displays the ^{13}C NMR spectra of the JFB. Short, methylated aliphatic compounds are thought to be present in the range of 0–30 ppm, while long, branched aliphatics are thought to be present in the range of 28–55 ppm. As a continuation of the former zone (the intermediate region), the range 45–85 ppm is thought to contain ethers, alcohols, phenols, and carbohydrates. This area contains nitrogen atoms (like pyridine) and carbon atoms next to oxygen atoms, similar to carbohydrates.

Aromatics and olefins are present in JFB in the range of 105–140 ppm. In addition to benzene-based chemicals, this area will also resonate with hetero aromatics that contain nitrogen and oxygen. There are carbonyl radicals present in the range of 165–182 ppm. The outcomes from the ^{1}H NMR and GC-MS are in harmony with the ^{13}C NMR estimate of the presence of different chemical components in JFB.

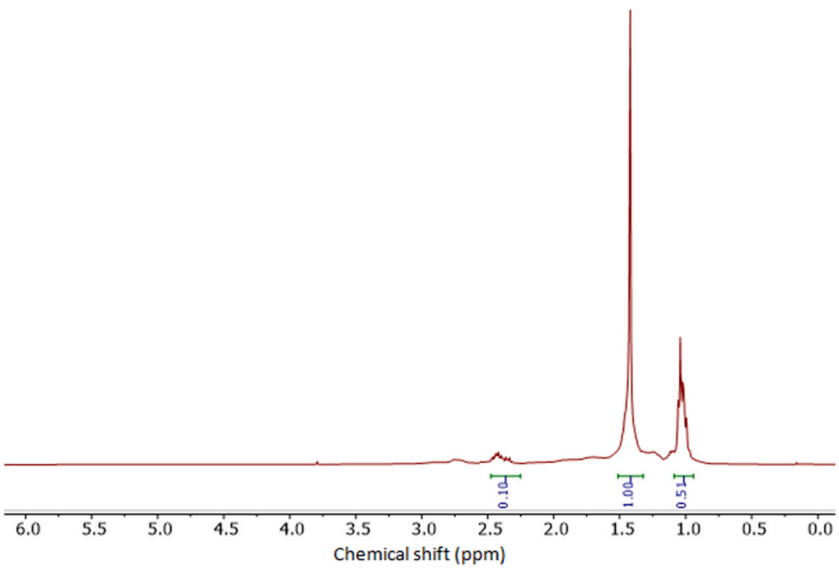

Fig. 14. 1H-NMR of JFB biodiesel.

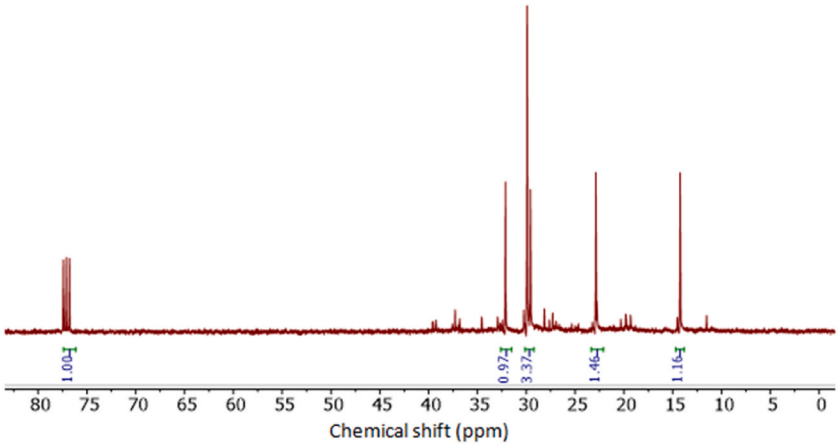

Fig. 15. ^{13}C-NMR of JFB biodiesel.

3.11. Rheological analysis

3.11.1. Effects of temperature on viscosity and shear stress of JFB (B100)

There is currently a paucity of research on the flow behavior of JFB in relation to shear stress and viscosity against temperature. The shear stress and viscosity relationships versus temperature are the main flow characteristics for any fuels and lubricants, so the present study carried out in this regard was based on different operating temperatures ranging from 20 to 65 °C. The relative shear stress is higher (0.55τ in Pa.s. at 20 °C) at low temperature while it is lower (0.1τ in Pa.s.at 65 °C) higher temperatures. The relative viscosity decreases with increasing temperature at a constant volume fraction of JFBO. This JFB has a fairly high viscosity at low temperatures (ranging from 10.589 Pa s at 20 °C to 1.737 Pa s at 65 °C) and decreased at high temperatures. Manufacturers of diesel engines, on the other hand, will not accept blends with viscosities below the range limit for diesel fuel. According to the standards, the minimum viscosity required for a biofuel to be utilized in a diesel engine is ranges from 1.9 to 4.9 cSt at 40 °C with the range recognized by ASTM D 6751as indicated in Ref. [81], based on this study the results obtained for the current JFB met the stated standard requirements. However, when the temperature rose, the viscosity and shear stress changed. In heat and mass transfer applications, where pumping power and viscosity-related problems this is a critical parameter. The sensitivity of viscosity to temperature and volume fraction of JFB fuel is demonstrated by variations in thermal conductivity that rise considerably with increasing temperature. Molecules having higher energy at higher temperatures resist intermolecular adhesive forces in liquid movement, particularly oils. As a consequence, as illustrated in Figs. 16 and 17, viscosity and shear stress decreased as temperature increased for JFB. The results show that when the temperature rises, the viscosity of the JFB decreases significantly. The inter-molecular distance between the JFBO grows as the temperature rises. As a result, the barrier to fluid layer flow decreases. Similar studies have also been shown by Refs. [82–85].

3.11.2. Effect of shear rate on viscosity

The viscosity profiles for JBF fuel is displayed in Fig. 18 using a rheological analysis at a constant operating temperature of 30 °C. The viscosity of juliflora biodiesel (B100) shows shear rate dependent behavior throughout a range of shear-thinning behavior over the shear rate of 10–150 s^{-1} with viscosity variation from 203.4 to 47.5 mPa s. After this stated shear rate range, the measured viscosity is almost unaffected with the shear rate effect till the completion of the applied shear rate.20 to 150 s^{-1}, although beyond this narrow shear rate range, the viscosity flow behavior is nearly shear rate-independent until the last 500 s^{-1} similar to the Newtonian behavior.

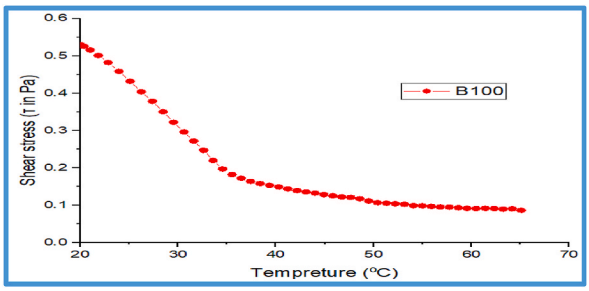

Fig. 16. Effects of temperature on shear stress for JFB.

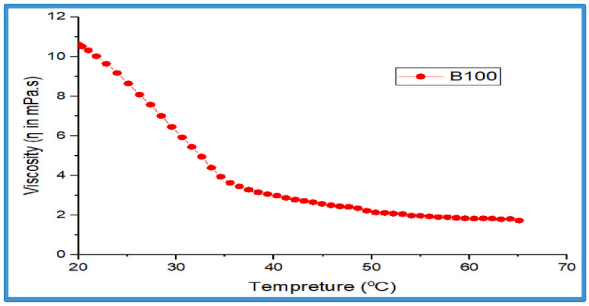

Fig. 17. Effects of temperature on Viscosities for JFB.

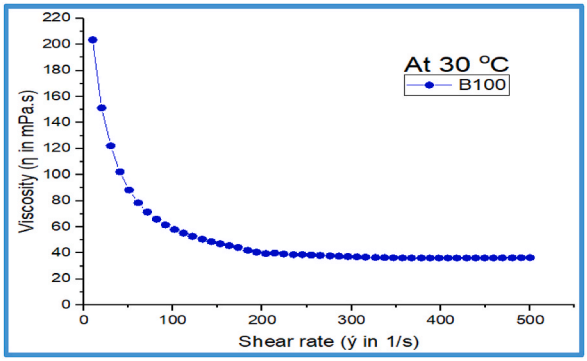

Fig. 18. Effect of shear rate on Viscosity.

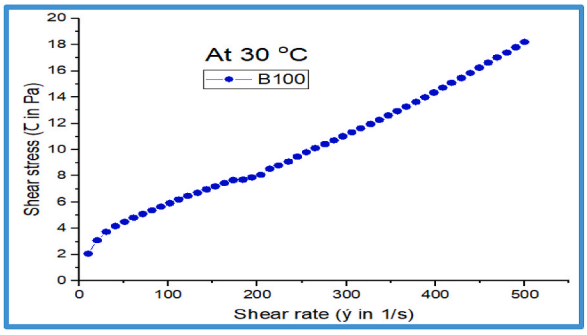

Fig. 19. Effect of shear rate on shear stress for JFB.

3.11.3. Effect of shear rate on shear stress for B100

Fig. 19 depicts the rheological behavior of the B100 JFB at a low constant operating temperature of 30 °C. The result reveals that as shear rate increases, the shear stress also tend to increase, the shear stress against shear rate exhibits almost linear correlations throughout the entire range of shear rate vs shear stress scales. The outcome may be used to characterize the flow behavior of the JFB that was tested. The tailored values of the flow behavior indicating that biodiesel with a higher shear rate increases shear stress at an increasing rate, as biodiesel with lower temperatures of 30 °C has higher viscosities. Because of the impact of the shear rate caused, and the lower temperature effect of 30 °C, the resultant flow behavior of the JFB (B100) may be linked to the intermolecular activities. Furthermore, the JFB (B100) fuel exhibits greater yield stress of 2.5 Pa at 10 $^{s-1}$.

4. Conclusion

1. The current study employs Prosopis Juliflora as a feedstock to produce, optimize, and characterize the resultant biodiesel. Complete characterization of Ethiopian variant JFB, not reported earlier has been done to identify functional groups, fatty acid compositions and the extent of aliphatic, olefin and aromatic compounds, This study will provide input to stakeholders and researchers interested

in alternative energy sources, provide alternative feedback for biodiesel, and turn the invasive JF species back into a useful approach to assist the national economy by substituting imported petroleum.

1. RSM was used to analyze the impact of time, catalyst concentration, methanol/oil ratio, and their interactions on biodiesel yield. As a result, the maximum biodiesel production of 87.5% was achieved under optimal conditions (methanol to ratio of 6:1, catalyst concentration of 0.5 wt at 55 °C, and period of 60 min). The agitation time for the Hexane solvent-crushed seed is 3 days with 480 ml of raw oil production at a maximum.
2. The FT-IR analysis reveals that JFB contains aliphatic groups of methyl esters, oxygen groups of ether and alcohol, unsaturated groups of alkenes, carbonyl groups of ester, nitrogen groups of amide and amine, and aromatic groups with various wavenumbers and transmittance intensity levels, all of which confirm that JFB meets the biodiesel requirements.
3. The GC-MS analysis of JFB reveals a carbon chain from C16 to C22 that contains different acids such as eurcic (68.81%), palmitic (2.08%), Oleic (4.15%), linoleic (5.77%), and linolenic (19.16%), all of which are biodiesel-compatible. Furthermore, even when not trans esterified into biodiesel, the produced oil has excellent and comparable properties to commercial biodiesel, including a high heating value (44.4 MJ/kg), density at 15 °C (0.894 g/ml), and kinematic viscosity at 40 °C (3.93), all of which meet the minimum requirements outlined in the American Standards for Testing Materials (ASTM 6751–3), indicating that biodiesel production with an eventual market entry is possible. The oil was Transesterified into biodiesel at a rate of 65%, paving the door for Juliflora biodiesel to be used in the biofuel sector. Producing biodiesel from JFB is technically feasible not just because this liquid biofuel is a "clean-burning fuel" that addresses pressing environmental concerns such as greenhouse gas reduction.
4. The NMR analysis reveled that the test result is in agreement with both the FT-IR and GC-MS findings. The different proton types: aliphatic, olefin, and aromatic compounds were exist in JFB at different ranges.
5. The Rheometer analysis depicts that as the temperature increases the viscosity and shear stress of JFB decreases linearly which means the oil confirmed Newtonian nature. The viscosity of juliflora biodiesel (B100) shows shear rate dependent behavior throughout a range of shear-thinning trait over the shear rate of 10–150 s^{-1} with viscosity variation from 203.4 to 47.5 mPa s, although beyond this narrow shear rate range, the viscosity flow behavior is nearly shear rate-independent until the last 500 s^{-1}.
6. This study scope is restricted to the production of biodiesel from PJF, optimization, its characterization and comparison with diesel fuel to ascertain parameter implications. The characterization of JFB is restricted to B100 and shows that certain of the properties of petro-diesel, such as density, kinematic viscosity, Cetane number, calorific value, and flash point, are comparable with JFB.
7. Previous studies related to JFB have not reported rheological analysis, cloud point, pour point, iodine value, free fatty acid (FFA), or copper strip degradation. Further studies on characterization and engine performance testing on JFB based B20 diesel, and DEE (diethyl ether) additive blended fuels can be pursued in the future.

Author contribution statement

Hailu Abebe Debella: Conceived and designed the experiments; Performed the experiments; Analyzed and interpreted the data; contributed reagents, materials, analysis tools or data; Wrote the paper. Venkata Ramayya Ancha, Samson Mekbib Atnaw: Conceived and designed the experiments; Analyzed and interpreted the data; Wrote the paper.

Funding statement

This research did not receive any specific grant from funding agencies in the public, commercial, or not-for-profit sectors.

Data availability statement

Data will be made available on request.

Declaration of interest's statement

The authors declare that they have no known competing financial interests or personal relationships that could have appeared to influence the work reported in this paper.

References

[1] A. Saravanan, M. Murugan, M. Sreenivasa Reddy, S. Parida, Performance and emission characteristics of variable compression ratio CI engine fueled with dual biodiesel blends of Rapeseed and Mahua, Fuel 263 (2020), 116751.
[2] T. Nguyen, M.H. Pham, T. Le Anh, Spray, combustion, performance and emission characteristics of a common rail diesel engine fueled by fish-oil biodiesel blends, Fuel 269 (2020), 117108.
[3] S.S. de Jesus, G.F. Ferreira, M.R. Wolf Maciel, R. Maciel Filho, Biodiesel purification by column chromatography and liquid-liquid extraction using green solvents, Fuel 235 (2019) 1123–1130.
[4] M. Athar, S. Zaidi, A review of the feedstocks, catalysts, and intensification techniques for sustainable biodiesel production, J. Environ. Chem. Eng. 8 (6) (2020), 104523.
[5] G. Bekele, W. Negatu, G. Eshete, Energy poverty in Addis Ababa city, Ethiopia, J. Econ. Sustain. Dev. 6 (3) (2015) 26–34.
[6] D.D. Guta, Assessment of biomass fuel resource potential and utilization in Ethiopia: sourcing strategies for renewable energies, Int. J. Renew. Energy Resour. 2 (1) (2012) 131–139.
[7] Z. Gebreegziabher, A.D. Beyene, R. Bluffstone, P. Martinsson, A. Mekonnen, M.A. Toman, Fuel savings, cooking time and user satisfaction with improved biomass cookstoves: evidence from controlled cooking tests in Ethiopia, Resour. Energy Econ. 52 (2018) 173–185.

[8] Ethiopia : Macroeconomic and Social Indicators, vol. 5, no. 1997, 2004.
[9] M. Bilal Tahir, K. Nadeem Riaz, A.M. Asiri, Boosting the performance of visible light-driven WO3/g-C3N4 anchored with BiVO4 nanoparticles for photocatalytic hydrogen evolution, Int. J. Energy Res. 43 (11) (2019) 5747–5758.
[10] D. Singh, et al., A comprehensive review of physicochemical properties, production process, performance and emissions characteristics of 2nd generation biodiesel feedstock: jatropha curcas, Fuel 285 (2021), 119110.
[11] M. Aghbashlo, S. Hosseinpour, M. Tabatabaei, Multi-objective exergetic and technical optimization of a piezoelectric ultrasonic reactor applied to synthesize biodiesel from waste cooking oil (WCO) using soft computing techniques 235 (2019) 100–112.
[12] S.S. Selvan, P.S. Pandian, A. Subathira, S. Saravanan, Comparison of response surface methodology (RSM) and artificial neural network (ANN) in optimization of aegle marmelos oil extraction for biodiesel production, Arabian J. Sci. Eng. 43 (11) (2018) 6119–6131.
[13] F. Ashine, et al., Biodiesel production from Argemone mexicana oil using chicken eggshell derived CaO catalyst, Fuel 332 (P2) (2023), 126166.
[14] P. Saravana Pandian, S. Sindhanai Selvan, A. Subathira, S. Saravanan, Optimization of aqueous two phase extraction of proteins from Litopenaeus vannamei waste by response surface methodology coupled multi-objective genetic algorithm, Chem. Prod. Process Model. 15 (1) (2020) 1–10.
[15] M. Anwar, M.G. Rasul, N. Ashwath, Production optimization and quality assessment of papaya (Carica papaya) biodiesel with response surface methodology, Energy Convers. Manag. 156 (2018) 103–112.
[16] P.R. Pandit, M.H. Fulekar, Egg shell waste as heterogeneous nanocatalyst for biodiesel production: optimized by response surface methodology, J. Environ. Manag. 198 (2017) 319–329.
[17] M. Anwar, M.G. Rasul, N. Ashwath, M.M. Rahman, Optimisation of second-generation biodiesel production from Australian native stone fruit oil using response surface method, Energies 11 (10) (2018).
[18] H. Chitsaz, M. Omidkhah, B. Ghobadian, M. Ardjmand, Optimization of hydrodynamic cavitation process of biodiesel production by response surface methodology, J. Environ. Chem. Eng. 6 (2) (2018) 2262–2268.
[19] M.A. Asokan, S. Senthur Prabu, P.K.K. Bade, V.M. Nekkanti, S.S.G. Gutta, Performance, combustion and emission characteristics of juliflora biodiesel fuelled DI diesel engine, Energy 173 (2019) 883–892.
[20] E. Raja, M. Premjeyakumar, Potent effect of prosopis juliflora (biodiesel + isopropanol + diesel) fueled with diesel engine and egr alteration, Clean. Eng. Technol. 4 (2021) 100205.
[21] R. Sasikumar, G. Sankaranarayanan, R. Karthikeyan, Investigation characteristics of prosopis juliflora biodiesel blended with diesel fuel in a DI diesel engine, Aust. J. Mech. Eng. (2020) 1–6.
[22] P. Felker, G. Cruz, K. Cadoret, The Prosopis Juliflora – Prosopis Pallida Complex, 2001.
[23] R. Chandran, R. Kaliaperumal, S. Balakrishnan, A.J. Britten, J. MacInnis, M. Mkandawire, Characteristics of bio-oil from continuous fast pyrolysis of Prosopis juliflora, Energy 190 (2020), 116387.
[24] S. Ramalingam, E. Murugesan, P. Ganesan, S. Rajendiran, Characteristics analysis of julifora biodiesel derived from different production methods, Fuel 280 (2020), 118579.
[25] S.G. Njokweni, P.J. Weimer, L. Warburg, M. Botes, W.H. van Zyl, Valorisation of the invasive species, Prosopis juliflora, using the carboxylate platform to produce volatile fatty acids, Bioresour. Technol. 288 (2019), 121602.
[26] A. Demirbas, Prediction of higher heating values for biodiesels from their physical properties, Energy Sources, Part A Recover. Util. Environ. Eff. 31 (8) (2009) 633–638.
[27] A. Demirbas. Biofuels Green Energy and Technology, Biofuel, 2009, 978. pp. 45-85, ISBN:978-1-84882-010-4.
[28] H. Shiferaw, et al., Modelling the current fractional cover of an invasive alien plant and drivers of its invasion in a dryland ecosystem, Sci. Rep. 9 (1) (2019) 1–12.
[29] W. Shiferaw, S. Demissew, T. Bekele, E. Aynekulu, Relationship between Prosopis juliflora invasion and livelihood diversification in the South Afar region, Northeast Ethiopia, Reg. Sustain. 1 (1) (2020) 82–92.
[30] T. Ramesh, A.P. Sathiyagnanam, M.V. De Poures, P. Murugan, Combined effect of compression ratio and fuel injection pressure on CI engine equipped with CRDi system using prosopis juliflora methyl ester/diesel blends, Int. J. Chem. Eng. 2022 (2022).
[31] T. Cornelissen, J. Yperman, G. Reggers, S. Schreurs, R. Carleer, Flash co-pyrolysis of biomass with polylactic acid. Part 1: influence on bio-oil yield and heating value, Fuel 87 (7) (2008) 1031–1041.
[32] T.T. Wakie, P.H. Evangelista, C.S. Jarnevich, M. Laituri, Mapping current and potential distribution of non-native prosopis juliflorain the Afar region of Ethiopia, PLoS One 9 (11) (2014) 3–11.
[33] M.M.K. Bhuiya, M. Rasul, M. Khan, N. Ashwath, M. Rahman, Industrial Crops & Products Comparison of oil extraction between screw press and solvent (n-hexane) extraction technique from beauty leaf (Calophyllum inophyllum L.) feedstock, Ind. Crop. Prod. 144 (2020), 112024.
[34] R. Huang, J. Cheng, W. Song, Y. Qiu, H. Guo, W. Yang, Physicochemical characterizations of microalgal methyl esters extracted with hexane and refined by vacuum distillation at different temperatures, Fuel 297 (2021), 120779.
[35] R. Huang, J. Cheng, Y. Qiu, Z. Zhang, J. Zhou, K. Cen, Solvent-free lipid extraction from microalgal biomass with subcritical water in a continuous flow reactor for acid-catalyzed biodiesel production, Fuel 253 (2019) 90–94.
[36] J. Cheng, R. Huang, T. Yu, T. Li, J. Zhou, K. Cen, Biodiesel production from lipids in wet microalgae with microwave irradiation and bio-crude production from algal residue through hydrothermal liquefaction, Bioresour. Technol. 151 (2014) 415–418.
[37] D. Singh, et al., A comprehensive review of physicochemical properties, production process, performance and emissions characteristics of 2nd generation biodiesel feedstock: jatropha curcas, Fuel 285 (2021), 119110.
[38] D. Singh, D. Sharma, S.L. Soni, S. Sharma, D. Kumari, Chemical compositions, properties, and standards for different generation biodiesels: a review, Fuel 253 (May) (2019) 60–71.
[39] E. Ozturk, Performance, emissions, combustion and injection characteristics of a diesel engine fuelled with canola oil-hazelnut soapstock biodiesel mixture, Fuel Process. Technol. 129 (2015) 183–191.
[40] A. Dhar, A.K. Agarwal, Performance, emissions and combustion characteristics of Karanja biodiesel in a transportation engine, Fuel 119 (2014) 70–80.
[41] M. Mofijur, H.H. Masjuki, M.A. Kalam, A.E. Atabani, I.M.R. Fattah, H.M. Mobarak, Comparative evaluation of performance and emission characteristics of Moringa oleifera and Palm oil based biodiesel in a diesel engine, Ind. Crop. Prod. 53 (2014) 78–84.
[42] B.K. Prajapati, A.S. Paikra, D.S. Mondloe, A Comparative Evaluation of Physical and Chemical Characteristics of Biofuel Synthesized from Kusum Oil (Schleichera Oleosa) and its Blends with Diesel, 2018, pp. 1066–1068.
[43] B. Ashok, et al., A novel study on the effect lemon peel oil as a fuel in CRDI engine at various injection strategies, Energy Convers. Manag. 172 (April) (2018) 517–528.
[44] Deresse Firew, N. Ramesh Babu, Mukesh Didwania, The performance evaluation of diethyl-ether (DEE) additive with Diesel blends using Diesel Engine test rig, Int. J. Sci. Eng. Res. 7 (6) (2016) 23–29.
[45] Zulqarnain, et al., Solvent extraction and performance analysis of residual palm oil for biodiesel production: experimental and simulation study, J. Environ. Chem. Eng. 9 (4) (2021), 105519.
[46] A.S. Silitonga, et al., A comparative study of biodiesel production methods for Reutealis trisperma biodiesel, Energy Sources, Part A Recover. Util. Environ. Eff. 39 (20) (2017) 2006–2014.
[47] K. Bhaskar, L.R. Sassykova, M. Prabhahar, M. Kiani Deh Kiani, K. Gomathi, S. Sendilvelan, Oxides of nitrogen and soot trade-off characteristics of methyl esters in a hybrid mode compression ignition engine, Mater. Today Proc. 45 (2021) 5847–5852.
[48] A.M. Ashraful, et al., Production and comparison of fuel properties, engine performance, and emission characteristics of biodiesel from various non-edible vegetable oils: a review, Energy Convers. Manag. 80 (2014) 202–228.
[49] P. Tamilselvan, N. Nallusamy, S. Rajkumar, A comprehensive review on performance , combustion and emission characteristics of biodiesel fuelled diesel engines, Renew. Sustain. Energy Rev. 79 (2017) 1134–1159.

[50] M.A. Asokan, S.S. Prabu, A. Bollu, M.A. Reddy, A. Ram, D.S. Sukhadia, Emission and performance behavior of hemp seed oil biodiesel/diesel blends in di diesel engine, Mater. Today Proc. 46 (2021) 8127–8132.
[51] A. Datta, B.K. Mandal, A comprehensive review of biodiesel as an alternative fuel for compression ignition engine, Renew. Sustain. Energy Rev. 57 (2016) 799–821.
[52] A.S. Roy, A. Chingkheihunba, K. Pakshirajan, An overview of production, properties, and uses of biodiesel from vegetable oil, Green Energy Technol (2016) 83–105.
[53] M. Krishnamoorthi, R. Malayalamurthi, The influence of charge air temperature and exhaust gas recirculation on the availability analysis , performance and emission behavior of diesel - bael oil - diethyl ether blend operated diesel engine 32 (4) (2018) 1835–1847.
[54] S. Krishnamoorthi, M. Prabhahar, V. Madhavan, T. Pragathish, F. Johnson, Effect of variation in injector nozzle holes on the Performance of preheated Spirulina methyl ester used in VCR engine, Mater. Today Proc. 45 (2020) 5840–5846.
[55] H. Mohamadzadeh Shirazi, J. Karimi-Sabet, C. Ghotbi, Biodiesel production from Spirulina microalgae feedstock using direct transesterification near supercritical methanol condition, Bioresour. Technol. 239 (2017) 378–386.
[56] D. Luning Prak, J. Cooke, T. Dickerson, A. McDaniel, J. Cowart, Cetane number, derived cetane number, and cetane index: when correlations fail to predict combustibility, Fuel 289 (2021), 119963.
[57] S. Sani, M.U. Kaisan, D.M. Kulla, A.I. Obi, A. Jibrin, B. Ashok, Determination of physico chemical properties of biodiesel from Citrullus lanatus seeds oil and diesel blends, Ind. Crop. Prod. 122 (2018) 702–708.
[58] D.M. Kulla, GC/MS Analysis of Methyl Esters of Biodiesel Produced from Cotton Seed Oil, 2016.
[59] P. Sivakumar, S. Sindhanaiselvan, N.N. Gandhi, S.S. Devi, S. Renganathan, Optimization and kinetic studies on biodiesel production from underutilized Ceiba Pentandra oil, Fuel 103 (2013) 693–698.
[60] P.K. Subramanian, P. Muthiah, Kinetic studies on oil extraction and biodiesel production from underutilized Annona squamosa seeds, Fuel 180 (2016) 211–217.
[61] S.S. Selvan, P.S. Pandian, A. Subathira, S. Saravanan, Saraca asoca seeds – a novel candidature for biodiesel production : studies on yield optimization using ANN coupled GA and properties of biodiesel blends, Int. J. Green Energy (2018) 1–12.
[62] D. de Almeida Cozendey, R. de Oliveira Muniz, R. Cavalcante dos Santos, C. Gimenes de Souza, D. Franca de Andrade, L. Antonio dAvila, Quantitative analysis of free glycerol in biodiesel using solid-phase extraction and high-performance liquid chromatography, Microchem. J. 168 (2021).
[63] D. Bisrat, S. Abate, and W. Kebede, Daniel Bisrat Solomon Abate Wossen Kebede Technical Manual 23 Manual for Plant Products Analysis.
[64] A.K. Azad, M.G. Rasul, M.M.K. Khan, S.C. Sharma, Biodiesel from Queensland Bush Nut (Macadamia Integrifolia), Elsevier Inc., 2017.
[65] I. Amalia Kartika, et al., Simultaneous solvent extraction and transesterification of jatropha oil for biodiesel production, and potential application of the obtained cakes for binderless particleboard, Fuel 181 (2016) 870–877.
[66] K. Bhaskar, et al., Analysis of Cymbopogon Citratus, Pinus sylvestris and Syzygium cumini biodiesel feedstocks for its fatty acid composition, Mater. Today Proc. 45 (xxxx) (2021) 5970–5977.
[67] G. Gnanashree, P.M. Sirajudeen, M. Sirajudeen, Determination of bioactive compounds in ethanolic extract of Caralluma indica using GC-MS technique, ~ 1675 ~ J. Pharmacogn. Phytochem. 7 (6) (2018) 1675–1677.
[68] G.P.P. Kamatou, A.M. Viljoen, Comparison of fatty acid methyl esters of palm and palmist oils determined by GCxGC–ToF–MS and GC–MS/FID, South Afr. J. Bot. 112 (2017) 483–488.
[69] A.C. Goren, G. Bilsel, M. Altun, F. Satil, T. Dirmenci, Fatty acid composition of seeds of Satureja thymbra and S. cuneifolia, Zeitschrift fur Naturforsch. - Sect. C J. Biosci. 58 (7–8) (2003) 502–504.
[70] S.H. Gowda, A. Avinash, K. Raju, Production optimization of Vateria Indica biodiesel and performance evaluation of its blends on compression ignition engine, Sustain. Chem. Pharm. 22 (2021), 100475.
[71] H.M. Xiao, S. Zhao, R.T. Fan, D. Hussain, X. Wang, Simultaneous determination of short-chain fatty alcohols in aged oil and biodiesels by stable isotope labeling assisted liquid chromatography-mass spectrometry, Talanta 229 (2021), 122223.
[72] C. Zhan, Z. Feng, W. Ma, M. Zhang, C. Tang, Z. Huang, Experimental investigation on effect of ethanol and di-ethyl ether addition on the spray characteristics of diesel/biodiesel blends under high injection pressure, Fuel 218 (2018) 1–11.
[73] N. Ivanova, V. Gugleva, M. Dobreva, I. Pehlivanov, S. Stefanov, V. Andonova, We Are IntechOpen , the World ' S Leading Publisher of Open Access Books Built by Scientists, in: For Scientists TOP 1%, i, Intech, 2016, p. 13.
[74] V. Prabhadevi, S.S. Sahaya, M. Johnson, B. Venkatramani, N. Janakiraman, Phytochemical studies on Allamanda cathartica L. using GC-MS, Asian Pac. J. Trop. Biomed. 2 (2 SUPPL) (2012) S550–S554.
[75] A. Gopinath, K. Sairam, R. Velraj, G. Kumaresan, Effects of the properties and the structural configurations of fatty acid methyl esters on the properties of biodiesel fuel: a review, Proc. Inst. Mech. Eng. - Part D J. Automob. Eng. 229 (3) (2015) 357–390.
[76] S.B. Sai, N. Subramaniapillai, M.S.B. Khadhar Mohamed, A. Narayanan, Effect of rubber seed oil biodiesel on engine performance and emission analysis, Fuel 296 (2021), 120708.
[77] A.E. Atabani, et al., Integrated valorization of waste cooking oil and spent coffee grounds for biodiesel production: blending with higher alcohols, FT–IR, TGA, DSC and NMR characterizations, Fuel 244 (2019) 419–430.
[80] R. Samantha and D. Almalik, "肖沉 1, 2, 孙莉 1, 2Δ, 曹杉杉 1, 2, 梁浩 1, 2, 程焱 1, 2," JNROnline J. ISSN2320-3358 ISSN0972-5547, vol. 3, no. 2, pp. 58–66, 2019, [Online]. Available: http://www.tjyybjb.ac.cn/CN/article/downloadArticleFile.do?attachType=PDF&id=9987.
[81] H. Lugo-Mendez, M. Sanchez-Dominguez, M. Sales-Cruz, R. Olivares-Hernandez, R. Lugo-Leyte, A. Torres-Aldaco, Synthesis of biodiesel from coconut oil and characterization of its blends, Fuel 295 (2021).
[82] J. Ma, A. Shahsavar, A.A.A.A. Al-Rashed, A. Karimipour, H. Yarmand, S. Rostami, Viscosity, cloud point, freezing point and flash point of zinc oxide/SAE50 nanolubricant, J. Mol. Liq. 298 (2020), 112045.
[83] P. Agarwal, S.K. Porwal, Non-edible/waste cooking oil–derived sustainable green multifunctional copolymeric additives for mineral base oil, Biomass Convers. Biorefinery 13 (4) (2021) 3017–3027, https://doi.org/10.1007/513399-021-01336-w.
[84] Q. Lei, F. Zhang, B. Guan, G. Liu, X. Li, Z. Zhu, Influence of shear on rheology of the crude oil treated by flow improver, Energy Rep. 5 (2019) 1156–1162.
[85] M.T. Ghannam, M.Y.E. Selim, Rheological properties of the jojoba biofuel, Sustain. Times 13 (11) (2021) 1–12.